coatings

MDPI

Review

Recent Developments in Accelerated Antibacterial Inactivation on 2D Cu-Titania Surfaces under Indoor Visible Light

Sami Rtimi *, Cesar Pulgarin and John Kiwi *

Ecole Polytechnique Fédérale de Lausanne, EPFL-SB-ISIC-GPAO, Station 6, CH-1015 Lausanne, Switzerland; cesar.pulgarin@epfl.ch

* Correspondence: sami.rtimi@epfl.ch (S.R.); john.kiwi@epfl.ch (J.K.); Tel.: +41-21-69-36150 (S.R. & J.K.)

Academic Editor: Naba Dutta

Received: 15 September 2016; Accepted: 23 January 2017; Published: 6 February 2017

Abstract: This review focuses on Cu/TiO_2 sequentially sputtered and $Cu\text{-}TiO_2$ co-sputtered catalytic/photocatalytic surfaces that lead to bacterial inactivation, discussing their stability, synthesis, adhesion, and antibacterial kinetics. The intervention of TiO_2, Cu, and the synergic effect of Cu and TiO_2 on films prepared by a colloidal sol-gel method leading to bacterial inactivation is reviewed. Processes in aerobic and anaerobic media leading to bacterial loss of viability in multidrug resistant (MDR) pathogens, Gram-negative, and Gram-positive bacteria are described. Insight is provided for the interfacial charge transfer mechanism under solar irradiation occurring between TiO_2 and Cu. Surface properties of 2D TiO_2/Cu and TiO_2-Cu films are correlated with the bacterial inactivation kinetics in dark and under light conditions. The intervention of these antibacterial sputtered surfaces in health-care facilities, leading to Methicillin-resistant Staphylococcus Aureus (MRSA)-isolates inactivation, is described in dark and under actinic light conditions. The synergic intervention of the Cu and TiO_2 films leading to bacterial inactivation prepared by direct current magnetron sputtering (DCMS), pulsed direct current magnetron sputtering (DCMSP), and high power impulse magnetron sputtering (HIPIMS) is reported in a detailed manner.

Keywords: magnetron sputtering; high power impulse magnetron sputtering (HIPIMS); bacterial inactivation kinetics; $Cu\text{-}TiO_2$ synergic effects; interfacial charge transfer (IFCT)

1. Introduction

The focus of innovative antibacterial materials is to find composites in colloid form or deposited on surfaces that are able to inactivate bacteria/pathogens within very short times and that have long operational lifetimes (high stability) [1–5]. Biofilms that spread bacteria in hospitals, schools, and public places are the most common and dangerous forms of infection by pathogens: bacteria, fungi, and viruses. Pathogens are capable of living in any environment where the minimal conditions of life are encountered, since they have the ability to form biofilms, adhering to each other and to surfaces. These pathogenic bacteria are continuously spread in closed environments, most commonly in health facilities [6–14]. Healthcare associated infections (HCAIs) are becoming a worldwide problem since bacteria can survive on abiotic surfaces for a long time. In this way, they disseminate a wide range of infections. The Center for Disease Control and Prevention (CDC) estimates that approximately two million patients/year are affected by HCAIs in the USA [15,16]. In Europe, HCAIs affect ~3.2 million patients/year, and lead to mortality or an increase of the duration of a hospital stay and associated costs [17]. Nosocomial infection occurs by simply touching the hands of healthcare workers or by hospital clothing, equipment, air conditioners, and hospital water distribution networks [18]. The use

of gloves, gowns, and masks, as well as patient isolation, have limited the spread of infections, but by themselves are not able to prevent the transmission of HCAIs [19,20].

The levels of contamination in UK hospitals have been reported to be ~10^5 CFU/cm^2 in diabetic wound dressing rooms, and in hospital residence rooms a density of 10^2 CFU/cm^2 was found. This review will address several studies on surfaces coated with TiO_2, Cu, and Cu/TiO_2 that have the potential to decrease the environmental bacterial density in hospital facilities. The added benefit of these coatings is that they avoid, to a certain degree, biofilm formation [21–26]. When HCAIs are caused by multidrug-resistant (MDR) pathogens this problem becomes critical, since antibiotics are not available or are ineffective due to their prolonged application times, making the pathogens resistant to their initially designed abatement effect.

At the present time, more work is required to improve antibacterial coatings that induce fast bacterial reduction, and have high adhesion, robust layered structures, and stability precluding HCAIs. The application of nanotechnology to produce innovative 2D biomaterial surfaces that are useful in medicine possesses a significant potential for the prevention and treatment of infections. Nevertheless, concerns exist about the use of these new nanoparticulate materials due to the incomplete knowledge of their toxicology [27,28].

The present write-up reviews the recent work on TiO_2, Cu, and the recent films made by Cu and TiO_2 that lead to fast bacterial inactivation kinetics precluding partial or total biofilm formation. The spread of pathogenic infections will be decreased depending on the type of pathogen or its local concentration. Biofilm formation is the origin of 80% of all microbial infections in the body, making biofilms a primary health concern [6–14]. Biofilm pathogens adhere to a host surface, organize their community structure, and remain there by producing an extra-cellular polysaccharides (EPS) polymer matrix to cement the biofilm to the support in a permanent way. In the present review, the co-sputtered films of Cu and Ti will be designated as Cu-TiO_2 and the sequentially sputtered films (TiO_2 sputtered first, followed by Cu sputtering) will be designated as Cu/TiO_2. We report Cu-TiO_2 inactivation of *E. coli* and Methicillin-resistant *Staphylococcus Aureus* (MRSA), a bacteria strain resistant to the effect of antibiotics and to a lesser degree, to the abatement of other bacteria. What makes the problem even more complicated is that bacteria embedded in a biofilm can survive concentrations of antiseptic/antibiotics that are several times higher than the concentration able to kill planktonic cells of the same species [29].

2. Bacterial Inactivation Performance on TiO_2/Cu and Surface Properties

2.1. Short Description of the Main Issues of Concern Affecting the TiO_2 Photocatalysis Application in Microbial Abatement

After the seminal report by Matsunaga et al. [30], a large number of papers appear devoted to the issue of microbial abatement in suspension or on supported TiO_2 surfaces. Lately, some reviews/monographs/reports have appeared on TiO_2 photocatalysis involving a large-scale effort addressed to: (a) the reporting of the references on TiO_2 photocatalysis; (b) the classification of the available data; and (c) proof of validity of the reported data by the recent reviews.

Foster et al. have reported on the TiO_2 mediated disinfection of a large variety of pathogens [31]. The main barriers to the application of TiO_2 photocatalysis in suspension have been recently reported by Guillard et al. [32], Morawski et al. [33], Robertson et al. [34], Dalrymple et al. [35], and Gamage et al. [36]. Reviews on the antimicrobial mechanism mediated by TiO_2 composite films and suspensions haves been reported by several groups such as Kubacka et al. [37] and Dalrymple et al. [38]. TiO_2, upon band–gap light irradiation, photogenerates charges that react with adsorbed O_2 and H_2O_{vapor} (at the solid-air interface), leading to reactive oxygen species (ROS) that present a high oxidation potential to degrade organic compounds and bacteria [39,40]. These (ROS) radicals are $HO^{\bullet}$, $O_2^{\bullet -}$, and $HO_2^{\bullet}$, and have been documented and characterized for most of their properties such as concentration, lifetimes, spectra, and redox potentials by numerous researchers. Linsebigler et al. [41], Nakano et al. [42], Fujishima et al. [43], Douad et al. [44], Griesser et al. [45], and Hu et al. [46] reported

the photocatalytic activity of TiO_2 thin films. However, more work using fast kinetics by femto- and picosecond spectroscopy in the visible region is still necessary to identify the nature and lifetime of these ROS species intervening in the individual pathogen inactivation. Recent works involving the fast kinetics of surfaces producing ROS under visible light that lead to subsequent *E. coli* inactivation have been reported recently by Kiwi et al. [47] and Rtimi et al. [48].

Photocatalytic degradation of pollutants and bacteria mediated by TiO_2 is a promising approach to face the increasing environmental contamination. However, because of its wide band gap (3.2 eV) TiO_2 can absorb mostly UV-light ($\lambda < 387$ nm) and only about 4%–5% of the visible radiation of the solar spectrum. Sensitization of TiO_2 modification by S or N anions, or metal/oxides such as Cu/CuO_x has been used to extend the TiO_2 response into the visible region. In this way, accelerated TiO_2 reaction kinetics under visible light, leading to bacterial inactivation on doped TiO_2, binary oxides, TiO_2 composites, or decorated 2D-surfaces, have been recently reported by Dionysiou et al. [49,50], Pillai et al. [51–53], Rtimi et al. [48], Kavitha et al. [54], Fotiou et al. [55], and Bahneman et al. [56].

Wettability plays an important role on the TiO_2 surface under band-gap irradiation. The surface wettability is evaluated by the water contact angle (CA). The CA (θ) is defined as the angle between the solid surface and the tangent line of the aqueous solution at the liquid-solid interface. Hashimoto, Fujishima, et al. [57,58] reported the importance of the hydrophilicity changes in TiO_2 under band-gap irradiation on the TiO_2 surface during pollutant/bacteria degradation. A hydrophobic TiO_2 surface at time zero was reported to become highly hydrophilic or superhydrophilic ($\theta < 5^\circ$) under band-gap excitation. This surface will gradually revert to the original surface after relatively long periods in the dark. This consideration is important in bacterial inactivation processes, since highly hydrophilic conversions lead to clean surfaces due to the destruction of bacteria adsorbed on the TiO_2 surface during the sample irradiation. The photo-generated holes have been shown to be responsible for the TiO_2 surface conversion to a highly hydrophilic surface. These holes (a) diffuse to the TiO_2 surface and to the oxygen lattice sites reacting with bacteria or (b) produce $HO^\bullet$-radicals reacting with the embedded $HO^\bullet$ on the TiO_2 surface. However, a part of the photo-generated holes break the –Ti–O– lattice bonds by coordinating H_2O at the Ti-lattice sites. The coordinated water releases a proton (charge compensation) and a new $HO^\bullet$ is formed, increasing the number of surface $HO^\bullet$ radicals [59].

Transparent, non-scattering PE (PE = polyethylene), sputtered by direct current magnetron sputtering (DCMS) for 8 min with TiO_2 thin film, inactivated *E. coli* within one hour under low intensity solar simulated irradiation (52 mW/cm^2). The scheme of the sputtering unit is shown in Figure 1. The PE was pretreated for 15 min by RF-plasma to graft a larger amount of polar negative groups able to bond the positive TiO_2 on the PE-surface [60–62]. The PE-TiO_2 samples pretreated for 15 min and sputtered for 8 min presented the highest amount of TiO_2 sites in exposed positions, leading to the favorable bacterial inactivation kinetics. A decrease from the initial contact angle (CA) of PE-TiO_2 at time zero and ~121 °C to $\theta < 5^\circ$ within 60 min of irradiation, inducing PE-TiO_2 super-hydrophilicity, was observed to be concomitant with the time of bacterial inactivation. This seems to be a necessary condition to attain the optimal *E. coli* inactivation kinetics. Samples sputtered for times >8 min led to a thicker coating, inducing charge bulk inward diffusion that decreased the charge transfer between the PE-TiO_2 and bacteria [63]. The rate of the hydrophobic to hydrophilic transformation was found to be 0.28 min^{-1}. The reverse reaction rate in the dark was found to be 8.7×10^{-3} min^{-1}. The reverse reaction time necessary to reach the initial hydrophobic CA ~121° was completed within about 24 h. These rates were calculated by integrating $\cos\theta$ in the Young's equation [58,59].

TiO_2 sputtering for 8 min led to a TiO_2 loading with the most suitable thickness for the charge diffusion generated in the TiO_2 to reach the bacteria. No bacterial re-growth was observed, meaning that there were no bacteria adhered to the surface after the inactivation cycle. After each cycle, the samples were washed with distilled water and dried. Then, the samples were kept in an oven at 60 °C to avoid bacterial contamination. After washing, the PE-TiO_2 samples were left standing for 24 h to regain the initial hydrophobicity.

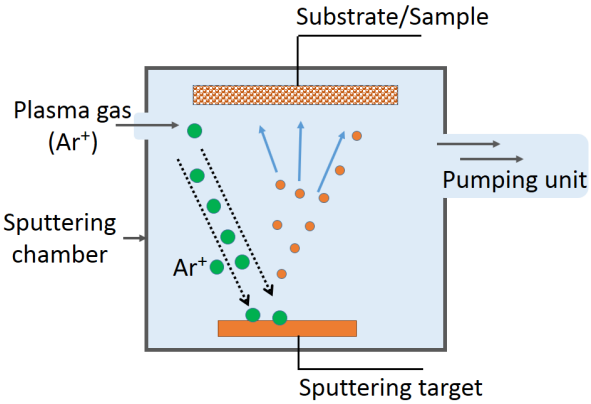

Figure 1. Sputtering unit used during the sputtering of antibacterial layers on diverse substrates.

According to Young's theory, the cosθ of a liquid droplet on a solid is a function of the interfacial energy between the solid and the liquid. The wettability is commonly evaluated in terms of the contact angle (CA), which is given by Young's equation [58]:

$$\gamma S = \gamma SL + \gamma L \cdot \cos\theta \quad (1)$$

In Equation (1), γS and γL are the surface free energies per unit area of the solid and the liquid, respectively, and γSL is the interfacial free energy per unit area. In addition, γSL can be approximated using the Girifalco-Good Equation (2), with γS and γL, as:

$$\gamma SL = \gamma S + \gamma L - \Phi(\gamma S/\gamma L)^{1/2} \quad (2)$$

Here, Φ is a constant parameter ranging from 0.6 to 1.1, depending on the solid. In addition, γL is the water surface free energy, which has a constant value of 74 mJ/m^2. Therefore, by combining Equations (1) and (2), the CA can be simply expressed as:

$$\cos\theta = c\gamma S^{1/2} - 1 \text{ (}c\text{: constant)} \quad (3)$$

The highly hydrophilic state generated by UV light gradually returns to the initial hydrophobic state in the dark. The initial contact angle on RF-pretreated DCMS sputtered PE-TiO_2 samples decreased to an angle < 5° within 60 min of irradiation. The hydrophobic or hydrophilic nature of a surface is important for the adhesion of bacteria to a TiO_2 layered surface and for regulating the subsequent light or dark induced kinetic bacterial inactivation.

E. coli and *Staphylococcus aureus* present a preferential adhesion to hydrophilic surfaces [32,64–67]. Efficient antimicrobial activity on Cu-surfaces has been recently reported against methicillin-resistant *Staphylococcus aureus* (MRSA) and the bacterial reduction was evaluated by four methods. A reduction of 4log$_{10}$ in the initial MRSA concentration of 10^6 CFU was found for ten clinical MRSA isolates within 1 h, suggesting the suitability of the Cu-surfaces in preventing the transmission of these gram-positive bacteria [64]. The loss of viability testing was performed by combining the data obtained by direct transfer on agar plates and stereomicroscopy. Two different methods were used to evaluate the bactericidal activity of the Cu-sputtered samples.

Bacteria with hydrophobic surface properties such as *S. epidermis* adhere preferentially to hydrophobic surfaces [66]. Hydrophobic bacteria such as *E. coli*, with an initial contact angle of 121° reduced to less than 5° (full hydrophilicity) have been reported within 5–10 min. *E. coli* was shown to adhere to Cu and TiO_2-Cu surfaces [40,46,60,61,67]. The negative charge on the catalyst/photocatalyst sputtered surface on TiO_2, TiO_2-Cu, and TiO_2-ZrO_2-polyester (PES) surfaces is outlined below in Equations (5)–(9):

$$\text{Bacteria} + [\text{PES-TiO}_2] + \text{light} \rightarrow [\text{PES-TiO}_2^*]\ \text{Bacteria} \rightarrow \text{Bacteria}^+ + \text{PES-(TiO}_2\text{)cbe-} \quad (4)$$

$$\text{PES-(TiO}_2\text{) cbe-} + \text{O}_2 + \text{H}^+ \rightarrow \text{HO}_2^\bullet \qquad E_0 \text{ -0.05 NHE [43,56]} \quad (5)$$

$$\text{PES-(TiO}_2\text{) cbe-} + \text{O}_{2\,\text{ads}} \rightarrow \text{O}_2^{\bullet -}{}_{\text{ads}} \qquad E_0 \text{ -0.16 NHE [43,56]} \quad (6)$$

$$\text{PES-(TiO}_2\text{) vbh}^+ + \text{OH}^-{}_{\text{ads}} \rightarrow \text{HO}^\circ \qquad E_0 \text{ -1.90 NHE [49]} \quad (7)$$

$$\text{PES-(TiO}_2\text{) vbh}^+ + \text{H}_2\text{O}_{\text{ads}} \rightarrow \text{HO}^\bullet{}_{\text{ads}} + \text{H}^+ \quad (8)$$

$$\text{O}_2^{\bullet -} + \text{H}^+ \Leftrightarrow \text{HO}_2^\bullet \qquad \text{pKa 4.8} \quad (9)$$

In reaction (2), the $HO_2^\bullet$ radical is stable at pH < 4.8, and above this pH, more than 50% is present in the form of $O_2^{\bullet -}$, as noted in Equation (9).

Most of the bacteria acquire a negative electric charge in aqueous suspension or in the presence of air humidity, and this aspect has been revealed to be important in bacterial adhesion to charged surfaces [68]. It has been known for a long time that surfaces with high surface energies, such as the ones encountered in hydrophilic surfaces, are to a great extent negative and develop resistance to bio-adhesion [69,70]. These two last considerations have to be considered from case-to-case when inactivating a specific pathogen on a well-defined antibacterial surface [6–13].

In the last 30 years, the TiO_2 mediated photocatalytic inactivation of pathogens has been the focus of bacterial disinfection studies. Inactivation by TiO_2 suspensions, supported photocatalysts, and nano-rods under diverse light sources has been reported within minutes/hours [71]. In dark control experiments, TiO_2 has been reported to exert no microbial inactivation or very low antibacterial activity. Recently, research has provided evidence that selected experimental conditions (pH, TiO_2 amount and particle size, bacterial concentration) below the TiO_2 isoelectric point led to 10^4 CFU/mL *E. coli* inactivation in the dark within 120 min. This was about 50% of the *E. coli* inactivation induced under the same experimental conditions when applying a UV-light centered at 366 nm. No photo-generated electrons/holes or ROS were present in the absence of band-gap irradiation [71]. This work showed that the electrostatic and or Coulomb interaction at pHs between 4 and 4.5 suppresses the division of bacteria leading to *E. coli* loss of cultivability.

A subsequent study presenting evidence for the lack of cultivability in the dark due to the interaction between TiO_2 surfaces in the minute range has been recently reported [72]. The bacterial cells interaction with TiO_2 aggregates was followed by electron microscopy. The interaction of the TiO_2 in the dark with *E. coli* led to cell wall damage/inactivation due to electrostatic forces competing with Van der Waals forces occurring at physiological pH-values and inducing damage/deformation in the cell-wall packing structure, with an increase of the membrane permeability. TiO_2-polyester samples demonstrated repetitive bacterial inactivation (loss of cultivability) in the dark. Bacterial inactivation in the dark occurred within 120 min compared to the *E. coli* mediated TiO_2 photocatalysis that occurred within 60 min under an actinic light Lumilux 18W/827 source (OSRAM GmbH, Winterthur, Switzerland), radiating within 350 and 740 nm, with an intensity of 4.1 mW/cm^2. This study reports on an important issue in the field of disinfection technology. The TiO_2-polyester led to disinfection processes being carried out in a repetitive way. This is a more convenient approach when compared to TiO_2 suspensions where the TiO_2 nanoparticles have to be removed from the solution after each cycle, not allowing for a continuous disinfection treatment. Therefore, TiO_2-supported polyester surfaces show a practical potential to preclude pathogenic biofilm formation in the dark. Alteration of the *E. coli* cell permeability in contact with TiO_2 in the dark has also been reported recently and the morphological changes of the bacteria were further documented by Guillard et al. [32]. The damage to the bilayer cell envelope was ascribed to the lipo-saccharide (LPS) packing structure damage. In contrast, SiO_2 under the same conditions did not induce detrimental effects on the bacteria, inhibiting its reproduction due to the variance of the electrostatic charges/interaction at the reaction pH. TiO_2 nanoparticles present a potential risk of these particles to penetrate in tissues and biological membranes. Ecotoxicology of TiO_2 has recently been addressed in several studies/reviews, which indicate the high stability of TiO_2 nanoparticles with limited cytotoxic effects [27,73–76].

The way light is applied to TiO_2 suspensions to inactivate bacteria has been reported recently in detail by Pulgarin et al. [77] to have significant effects on the inactivation kinetics. The way

light is applied during bacterial disinfection may or may not lead to complete bacterial removal: continuous irradiation leads to a rapid removal of bacteria compared to the same light dose applied intermittently. No bacterial re-growth was observed after illumination of a contaminated TiO_2 suspension. In contrast, without catalyst, illuminated bacteria in solution recovered their initial concentration after 3 h in the dark. In a subsequent study, TiO_2 suspensions were shown to be effective in reducing *E. coli* when irradiated in the presence of a bacterial consortium. The inactivation rate was dependent on biological parameters such as physiological state, pH, initial concentration of bacteria, and the organic/inorganic impurities/residues present in the solution. After illumination periods with different lengths, a "residual disinfecting effect" in the dark was observed after the light was turned off, as a function of the applied intensity (40–100 mW/cm^2). *Enterococcus* sp., a Gram-positive bacterium with cell-wall thicknesses between 30 and 80 nm appear to be less sensitive compared to coliforms and other Gram-negative bacteria with cell-wall thicknesses 10–20 nm to the effect of TiO_2 under light [78].

Generally, the bacterial inactivation kinetics is determined by the hydrophobic-hydrophilic properties of the surface mediating the bacterial disinfection. For different processes involving TiO_2 surfaces, the hydrophobic-hydrophilic conversion in air under solar light irradiation proceeds with shorter times compared to the time required for *E. coli* inactivation. References [79,80] by Rtimi et al. show that initial hydrophobic PE-TiO_2 surfaces under solar simulated irradiation became super-hydrophilic surface within times <1 h. The conversion of the initial hydrophobic surfaces (contact angle >150°) to super-hydrophilic surfaces (contact angle <5°) is accepted as a necessary condition but not the only necessary condition for bacterial inactivation on PE-TiO_2 surfaces. The PE-film presents a smooth surface that allows the measurement of sputtered TiO_2 by applying different powers and conveniently follows the change in the dynamic contact angle measurements with time [81].

In TiO_2 dispersions/suspensions made up of colloids or pre-formed powder nanoparticles, the photocatalysis led to many studies focusing on bacterial abatement [12,30–63,71,72] and showing the inactivation of spores [82–85], viruses [86], algae [87], and fungi [88]. The TiO_2 suspensions, although successful in abating a variety of pathogens under light irradiation, require times that seem to be too long to treat large water volumes. The second inconvenience is the separation of the suspension from the bacterial residues after the disinfection process. This is expensive in terms of time, labor, and reagents. Therefore, some laboratories have begun to use supported TiO_2 materials in disinfection processes mediated by TiO_2. To avoid the separation step at the end of the bacterial abatement, Kuhn et al. [89] reported in 2003 that preformed TiO_2 nanoparticles grafted on plexiglass surfaces inactivate *E. coli* under UV-light, but only to a small extent. Nevertheless, these surfaces showed a very heterogeneous (non-uniform) TiO_2 coating. Generally, coating with colloidal TiO_2 on thermal resistant substrates such as glass, iron plates, and ceramics provide layers that are not reproducible and can be wiped off by rubbing using naked hands [90].

The synthesis of uniform 2D-coatings on supports by applying direct current magnetron sputtering (DCMS), pulsed direct current magnetron sputtering (DCSMP), and highly ionized pulsed plasma magnetron sputtering (HIPIMS) have been reported to uniformly cover surfaces resistant to thermal stress. However, sputtering methods have been used to coat textiles such as cotton and polyester (PES) and low cost inert thin polymer films such as polyethylene (PE) that present low thermal stability $\leq$100–130 °C comprise 80% of the commercial market.

2.2. TiO_2/Cu Synthesis Leading to Uniform, Adhesive, and Antibacterial Films

Physical vapor deposition (PVD) is carried out in a vacuum by condensation of a metal/non-metal vapor onto the support surface that is generally in the reaction chamber at a relatively low temperature. This method involves high temperature vacuum evaporation of the material to be coated on the support. Anatase layers have been deposited in this way, showing a super-hydrophilic behavior under band-gap irradiation as reported by several researchers in the field [91]. When using chemical vapor deposition (CVD), the substrate is exposed to volatile compounds that decompose on the substrate,

leading to the desired coatings [92–94]. A uniform, thin, adhesive, robust TiO_2 film has been deposited on glass [95] from Ti-chloride/ethyl-acetate at about 500 °C. CVD is able to deposit continuous films without the need of a post-annealing process to crystallize the TiO_2 nanoparticulates.

Diverse pulse magnetron sputtering (PMS) systems have been used to deposit TiO_2 films with thicknesses of up to 300 nm and layers comprising mainly anatase at temperatures $\leq$130 °C. Using this approach, textiles presenting low thermal resistance, thin polymer films, and polycarbonates (PC) have been coated with TiO_2, TiO_2-metal, and TiO_2 metal-oxides [61,96–98]. The basic installation of a DCMS unit is shown in Figure 1.

One of the first reports on DCMS sputtered photocatalytic TiO_2 on Si-wafers and ceramic targets was reported by Miron et al. [99]. The utility of TiO_2 sputtered surfaces was already recognized many years ago. During the photocatalytic disinfection, the electron acceptor, O_2, in contact with the sputtered TiO_2, is readily available from the air and its concentration is normally replenished by the catalyst surface during disinfection. The efficiency of the antibacterial catalytic surface is influenced by the surface porosity, the intensity of the light, the sample roughness and uniformity, the type of bacteria (either Gram-negative or Gram-positive), the distance of the light source to the sputtered sample, the surface pH, and the hydrophilic-hydrophobic balance of the sputtered sample.

2.3. Cu-Loaded Sputtered Surfaces Active in the Dark and under Light, Leading to Microbial Abatement

Antimicrobial nanoparticulate films preparation is a topic of increasing attention since its objective is to reduce or eliminate the formation of infectious bacteria biofilms leading to hospital acquired infections (HAI) [100]. However, more effective bacterial inactivation films on flat or complex 2D/3D surfaces are needed due to the increasing resistance of pathogenic bacteria to synthetic antibiotics administered for long periods of time. Additionally, nosocomial infections due to antibiotic resistant bacteria are becoming more frequent [25]. Surfaces sputtered by DCMS/DCMSP containing metals, oxides, or semiconductors (either heat resistant or not) have been reported recently, leading to effective, stable, and uniform bactericide films [101–103]. The recently developed highly ionized pulsed plasma magnetron sputtering (HIPIMS) leads to films by applying high electrical pulses of 1–10 A and up to 100 V, which leads to layers that present superior resistance and compactness against corrosion and oxidation. The HIPIMS sputtering on 3D-complex objects addresses the problems encountered when depositing thin films on substrates by DCMS/DCMSP [102] since the adhesion of the sputtered films (by DCMS/DCMSP) is not very strong. This is due to the relatively low bias voltage applied on the substrate during the sputtering time [103]. HIPIMS sputtering induces a strong interaction with 2D/3D substrates due to the higher fraction of the Cu^+/Cu^{2+}-ions; up to 70% compared with DCMS/DCMSP [104]. The Cu-ions generated by DCMS were reported by Castro et al. [105] and by using X-ray Photo-electron Spectroscopy (XPS), evidence was shown for the Cu^+/Cu^{2+} and Cu^{3+} ions. Subsequently, a larger amount of Cu-ions was reported on a support by Osorio et al. after applying DCMSP [106]. More recently, a study using HIPIMS reported by Rtimi et al. [107] led to a significantly higher amount of Cu-ions on the Cu-PES surfaces, accelerating bacterial inactivation compared to DCMS and DCMSP. The relatively lower sputtering energies employed during DCMS and DCMSP sputtering would at first sight be a reason to expect a higher amount of Cu-ions being able to leave the Cu-PES surface and interact/stick to the outer cell wall of *E. coli*, and then diffuse through the porins and translocate to the cytoplasm, inducing bacterial inactivation/death. However, the opposite effect was observed. HIPIMS sputtering ionized 70% of the $Cu^{\bullet}$ to Cu-ions in the HIPIMS chamber, leading to highly charged Cu-ion surfaces. The higher amount of Cu-ions later translocated through the *E. coli* porins, inducing an accelerated bacterial inactivation [108].

The strong adherence of the sputtered atoms/ions on complex shape biased objects is due to the higher ion-arrival energy on the surface compared to the more traditional DC/DCP sputtering methods [104]. Cu-ions in ppb-amounts, besides electrostatically interacting with the bacterial envelope, lead to the partial unpacking/damage of the LPS of the outer *E. coli* bacterial cell wall, later penetrating the bacterial cell-porins with diameters of 1.1–1.3 nm [109]. Cu-ions will

also diffuse through skin pores of ~100 nm [6,12,27–31]. To preclude the viral and diverse types of nosocomial infections caused by antibiotic resistant bacteria, Borkow and Gabbay have reported studies on Cu-loaded textiles [110–113]. These studies report in a detailed, systematic, and comprehensive way the preparation and evaluation of the pathogen abatement on these innovative surfaces. Furthermore, colloidal Cu-coated textiles showing antibacterial properties were reported by Gedanken's group [114,115], focusing on ZnO and CuO colloids deposited on textiles by sonication. Cu-colloids were impregnated on polyester (PES) to inactivate bacteria under low intensity sunlight. The PES was previously pre-treated by RF-plasma to increase the amount of negative carboxylic sites able to bond to Cu-ions [116]. The non-uniform dispersion of the Cu/CuO_x on the PES surface motivated us to work on the preparation of Cu-antibacterial films by sputtering in order to obtain adhesive, uniform, and reproducible Cu/CuO_x coatings. In this way, we overcame the shortcomings of colloidally loaded PES and this work will be described in the paragraph below.

DCMS prepared samples were carried out with Cu-targets (99.9%) from Lesker AG, Hastings, East Sussex, UK, and the textiles/thin polymer films were sputtered in a magnetron chamber at a pressure of 0.1–1 Pa. The distance between the Cu-target and the substrate was ~10 cm, the deposition current was 30–250 mA, and the voltage was varied between 100 and 500 V. The Cu-film thickness was determined with a profilometer (Alphastep500, Tencor, Rocklin, CA, USA). Cu-DCMS sputtered for 40 s formed a 3 nm thick film (or 15 atomic layers) and led to the fastest *E. coli* inactivation [105]. The most favorable structure-reactivity Cu-cluster agglomerates sputtered on cotton is defined as the Cu-nanoparticulate on cotton, and led to the most favorable bacterial inactivation kinetics. During several studies on Cu, CuO, and Cu/TiO_2 sputtered nanoparticulates, it was shown that the Cu-sputtering time or the amount of Cu sputtered on the substrate did not directly relate to the bacterial inactivation time [105–107,117–119]. From this it was concluded that the Cu-ions play an important role in mediating bacterial disinfection and these Cu-ions were determined by X-ray photoelectron spectroscopy (XPS).

The magnetic sputtering chamber contains Ar that upon impact of the applied current ionizes to Ar^+

$$Ar \rightarrow Ar^+ + e^- \text{ or } Ar^* + e^- \quad (10)$$

$$Ar^+ + Cu^\bullet \rightarrow Cu^+ + Ar^\bullet \quad (11)$$

$$e^- + Cu^\bullet \rightarrow Cu^+ + 2e^- \quad (12)$$

In Equation (12), the direct electron impact of highly energetic/high speed electrons kicks off an e^- of the Cu-target. The intensity of the e^- collision with the $Cu^\bullet$-target is proportional to the energy/current applied in the sputtering chamber. The Ar may also attain only excited states and ionize the $Cu^\bullet$, as shown in Equation (13), because the Ar has a higher energetic content than the ionization energy necessary to ionize CuO by a process called penning ionization:

$$Ar^* + Cu^\bullet \rightarrow Cu^+ + Ar + e^- \quad (13)$$

The Cu ions produced in the Ar-plasma are accommodated on the substrate, leading to Cu-films by epitaxial growth through nucleation, followed by growth that leads to atomic clusters/agglomeration/crystals that present metal/oxide character depending on their size and the growth symmetry [21,117,120]. The condensation of Cu and Cu-ions necessary to form Cu-films on the substrate involve the preference of Cu-atoms for binding to other Cu-atoms/ions rather than to the substrate, leading to agglomerates [121,122]. Depending on the Cu-sputtering time and energy, Cu-clusters are formed that are not necessarily crystallographic, which depend on the affinity between the Cu-atoms and the substrate. During the Cu-atom/ions condensation/coalescence during the formation of the film, sometimes the Cu-nuclei merge on the substrate without forming grain boundaries [123,124].

Once the Cu clusters/atoms are on the surface of a substrate, they interact with O_2 which leads to CuO or Cu_2O [105–107,117,119–122,125–131]. The oxidative state of the nanoparticulate Cu determines the bacterial mechanism/kinetics. The semiconductor character of CuO allows for the generation of photo-induced charges. The amount of these species is a function of the applied light dose. The CuO and Cu_2O mechanistic steps inducing charge separation under band-gap irradiation, leading subsequently to bacterial inactivation, could be suggested as:

$$CuO + h\nu \text{ (sunlight)} \rightarrow CuO(cbe^-), CuO(vbh^+) \quad (14)$$

where $CuO(cbe^-)$ refers to the conduction band electrons generated and the CuO-semiconductor under band-gap irradiation, and $CuO(vbh^+)$ are the holes generated concomitantly in the CuO-valence band. Under photon energies exceeding the CuO band-gap, the cbe^- electron could either react directly with the O_2, forming $O_2{}^-$, or reduce the Cu^{2+} to Cu^+ as suggested below:

$$CuO(cbe^-) + O_2 \rightarrow CuO + O_2{}^- \quad (15)$$

$$CuO(cbe^-) \rightarrow CuO(Cu^+) \quad (16)$$

$$CuO(Cu^+) + O_2 \rightarrow CuO(Cu^{2+}) + O_2{}^- \quad (17)$$

The cbe^- in Equation (17) is produced by a CuO (p-type) with a band-gap energy of 1.7 eV, a flat-band potential of −0.3 V SCE (pH 7), and a valence band at +1.4 V SCE [56].

$$CuO(Cu^+) \rightarrow CuO \text{ vacancy} + Cu^+ \quad (18)$$

$$CuO(vbh^+) + \text{bacteria} \rightarrow CO_2, H_2O, \text{inorganic N,S} \quad (19)$$

The photocatalytic reactions for the Cu_2O mediated bacterial inactivation are suggested in Equations (20)–(23). The highly mobile electrons first transfer from $Cu_2O(cbe^-)$ to the TiO_2cb as suggested in Equation (21).

$$Cu_2O + h\nu \rightarrow Cu_2O(cbe^-), Cu_2O(vbh^+) \quad (20)$$

$$Cu_2O(cbe^-) + TiO_2 \rightarrow TiO_2{}^- \text{ or } (Ti^{3+}) \quad (21)$$

$$TiO_2{}^- + O_2 \rightarrow TiO_2 + O_2{}^- \quad (22)$$

$$Cu_2O(vbh^+) + \text{bacteria} \rightarrow CO_2, H_2O, \text{inorganic N,S} \quad (23)$$

Taking 0.3 nm as the distance between the Cu-atoms on the film surface and the thickness of an atomic layer ~0.2 nm, a Cu-coating 20 nm thick (about 100 layers) was deposited by DCMS for 20 s with a content of 1×10^{17} Cu atoms/cm^2 at a rate of 5×10^{15} atoms/cm^2·s.

DCMSP of Cu with energy pulses between 5 and 15 eV led to faster bacterial inactivation kinetics compared to DCMS [106]. More recently, higher energies per pulse compared to DCMSP involving HIPIMS sputtering was reported by Petrov et al. [104]. HIPIMS sputtering on Cu-PES led to *E. coli* bacterial inactivation within 90 min when Cu was sputtered by HIPIMS pulses that were 60 s long at 60 A [117]. Effective bacterial inactivation was also observed in the dark. The energy and duration of the HIPIMS pulse was also limited by the heat resistance of the Cu-target. The amount of Cu-sputtered by HIPIMS inactivated *E. coli* with a Cu-loading three times lower that that compared to DCMS, leading to *E. coli* bacterial inactivation within similar times. This demonstrates substantial Cu-metal savings when using Cu to prepare Cu-HIPIMS antibacterial films. A higher amount of Cu-ions was detected by X-ray photoelectron spectroscopy (XPS) on the textile surface for HIPIMS sputtered films compared to films sputtered by DCMS and DCMSP [64,105,106,117].

2.4. Behavior of Cu-Sputtered Surfaces in the Dark and under Hospital Settings (Indoor Actinic Light), Leading to MRSA-Isolate Inactivation

Studies showing the reduction of the bacterial load on various Cu-surfaces are of growing interest regarding indoor environments. Figure 2 shows a simplified scheme for bacterial inactivation mediated by Cu/CuO under light irradiation. Cu-particles are covered by CuO when exposed to air and present semiconductor behavior, leading to the separation of charges that induces bacterial inactivation under light. This mechanism has been accepted during the last three decades addressing the bacterial inactivation by CuO as shown in Figure 2.

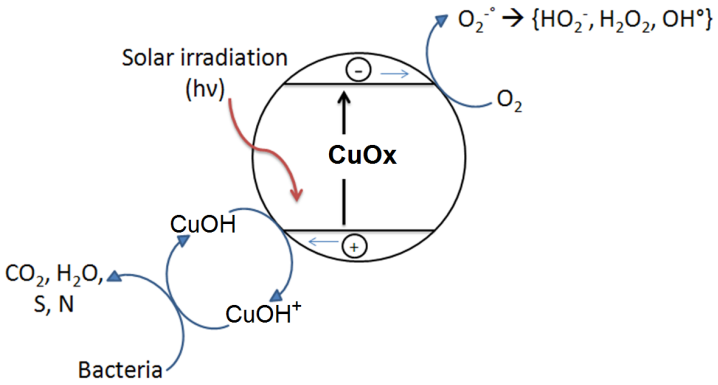

Figure 2. Conventional bacterial inactivation model on PE-CuO_x films under solar light irradiation.

The inactivation of Vancomycin resistant enterococci (VRE) and MRSA isolates is important due their strong infectious effects and the fact that they can survive for months in health facilities [6–14,23–26]. The inactivation of multidrug-resistant (MDR) pathogens such as Gram-positive, Gram-negative, or fungi on Cu-polyester (Cu-PES) has been reported [132,133]. The DCMS of Cu was carried out on polyester (PES) for different times and led to uniform adhesive Cu nanoparticulate films. Cu-PES samples sputtered for 160 s were observed to induce a $6\log_{10}$ CFU loss of viability for MRSA and *A. baumanni* within 30 min. The loss of bacterial viability on the Cu-PES surface for other MDR bacteria proceeded with similar times in dark/light conditions, suggesting that Cu/Cu-ions and not CuO_x led to the observed bacterial loss of viability. The use of gloves, gowns, and masks, as well as patient isolation, have limited the spread of infections, but on their own are not able to avoid the transmission of HCAIs [134,135].

Copper is required by eukaryotic and prokaryotic cells at low concentrations as cofactors in metal-proteins and enzymes, but at high concentrations, Cu-(II) has a toxic effect. Cu intervenes by substituting essential ions and blocking the functional groups of proteins, inactivating enzymes, which produces highly oxidative free radicals such as $HO^{\bullet}$, $HO_2^{\bullet}$, and $O_2^{-\bullet}$ which damages the membrane integrity [30–40]. A number of studies have demonstrated the efficient killing of bacteria/fungi on Cu-surfaces and Cu-alloys, both in vitro and in a clinical setting; Espirito Santo et al. [136,137], Grass et al. [138], and Casey et al. [139]. These studies show that Cu-surfaces rapidly and efficiently kill bacteria, in some cases accumulating Cu-ions on the cell wall membranes. This step seems to be followed by Cu-uptake, leading to loss of integrity of the cell wall and Cu-translocation. These studies also report that Cu/Cu-ions are effective against a wide variety of microbes, but the mode of intervention of the Cu/Cu-ions and the inactivation mechanism still remains controversial. Experimental evidence for reactive oxidative stress (ROS) on the cytoplasm of Cu-stressed yeast has been presented. New biomaterials consider additives that interfere with biofilm formation, adhesive properties, and involve a microstructure driving the antibacterial action [13]. Testing the antibacterial action of many metals on TiO_2 films, the metal-ion toxicity of Cu-ions was found to be much higher compared to Ag-, Zn-, Co-, Al-, and Hg-ions. The in vitro growth inhibition revealed

the higher activity of Cu-ions as an antibacterial and bio-tolerant additive in ppb amounts [140]. Due to the fact that many bacteria grow easily on polyethylene that is widely used to wrap all kinds of objects: pharmaceuticals, perishables, and surgical materials by Cu-polyethylene (Cu-PE) thin polymeric films, our laboratory decided to sputter Cu on PE by DCMS and test its bacterial inactivation performance [141]. Cu-coatings of 25 nm thickness were sputtered at 60 W and deposited 0.16% weight Cu/weight PE, leading to bacterial inactivation under low intensity simulated sunlight (20% the solar irradiation reaching the equator at noon presenting 100 mW/cm^2). These films were also able to induce complete bacterial inactivation in the dark within 90 min and at a faster rate within 15 min under low intensity sunlight. Repetitive photo-induced bacterial inactivation was observed on the CuO_x-PE. The Cu released in the ppb-range during the catalyst recycling was determined by inductively coupled plasma mass-spectrometry (ICP-MS). An increase in the applied light intensity accelerated the bacterial inactivation kinetics, providing evidence for the semiconductor behavior of the CuO_x film. Using X-ray photoelectron spectroscopy (XPS), the binding energy (BE) of the Cu-species was observed to shift after the bacterial inactivation cycle, providing evidence for redox processes during bacterial inactivation.

The use of intravenous catheters (IVCs) in patients who require vascular access is often associated with the development of potentially severe infections, including bloodstream infections (BSI), metastatic abscesses, and infective endocarditis [142,143]. Catheters are commonly colonized by microorganisms present on the skin at the time of intravascular insertion [144]. The infections caused by staphylococci, such as *Staphylococcus aureus*, are problematic in the case of methicillin-resistant *S. aureus* (MRSA) [145]. Polyurethane catheters currently used in Swiss hospitals do not generally have an infection during the first day, but are prone to infections when used for longer hospital periods [23–25,100,112,133,135]. Catheters (being 3D-objects) were sputtered by Ag-Cu and the substrate/sputtered film was maintained under a negative bias of 100–200 V. The Ag/Cu-coatings sputtered led to a faster bacterial inactivation compared to either Ag or Cu by themselves. The layers presented a thickness of ~30 ± 3 nm (150 layers) on the catheters. The antibacterial coatings were investigated for their efficacy in preventing MRSA infections in vitro and in vivo [145]. Ag and Cu were sputtered (67%/33% ratio) externally on polyurethane catheters by DCMS. In vitro, Ag/Cu-coated and uncoated catheters were immersed for 18 h at 4 °C in PBS or rat plasma and exposed to 10^4–10^8 CFU of MRSA ATCC 43300 for 90 min at 37 °C. In vivo, Ag/Cu-coated and uncoated catheters were placed in the jugular vein of rats. Nearby, MRSA (10^7 CFU) was inoculated in the tail vein. Catheters were removed 48 h later and cultured. In vitro, Ag/Cu-coated catheters that were pre-incubated in phosphate buffered saline (PBS, a biological media used routinely in bacterial testing) and exposed to 10^4–10^7 CFU, prevented the adherence of MRSA (0%–12% colonization) compared to the uncoated catheters (50%–100% colonization; $p < 0.005$). When pre-incubated in rat plasma, Ag/Cu-coated catheters retained their activity (0%–20% colonization) while the colonization of uncoated catheters increased (83%–100%; $p < 0.005$). Ag/Cu-coating protection decreased with 10^8 CFU in both PBS and plasma (50%–100% colonization). For the in vivo experiments, Ag/Cu-coated catheters reduced the incidence of catheter infection compared to uncoated catheters (79% vs. 57%, respectively) and bacteraemia (68% vs. 31%, respectively; $p < 0.05$). Scanning electron microscopy (SEM) of explanted catheters suggests that the Ag/Cu catheters formed a dense fibrin sheath over their surface in vivo, hindering the access of Ag/Cu to the infecting staphylococci. Their activity might be improved by limiting plasma protein adsorption on their surface. The Ag/Cu-coating of catheters completely prevented catheter infection by MRSA in vitro.

Due to the interest of the subject and the recent advances in the Cu-inactivation of pathogens, several studies have addressed this area and have reported incipient results on Cu-mediated disinfection processes [146–154].

2.5. Photocatalytic/Catalytic Bactericidal Effects on E. coli and MRSA by TiO_2/Cu Thin Films

In the last decade, Cu has been widely reported to increase the bactericidal activity of TiO_2 [13,22,42,43,56,64,94,112–115,132–142,153]. This section presents some relevant developments

(and references) of work regarding bacterial inactivation mediated by TiO_2/Cu powders and TiO_2/Cu surfaces by catalysis and photocatalysis. Doping/decorating TiO_2 by Cu/CuO_x enhances the visible light absorption of TiO_2 and it has also been suggested to enhance the charge separation. The speciation of Cu on the TiO_2 surface and the mechanism of interfacial charge transfer (IFCT) between TiO_2 and Cu remains a controversial matter.

Inactivation of bacteria under UV and visible light on TiO_2/Cu has been reported by the group of Applied Chemistry, University of Tokyo in the seminal references [155–158]. Hashimoto's laboratory has published studies on the preparation of TiO_2/Cu nanoparticles by sol-gel methods and have evaluated their performance under UV and visible light. Under weak UV-indoor lighting, they demonstrated a notable activity increase of bacterial inactivation by the TiO_2/Cu films (40 $\pm$ 4 nm) with respect to TiO_2-films. The observed effect was ascribed to the ROS generated under band-gap irradiation, which first attacked/damaged the LPS *E. coli* outer membrane, followed by the effective uptake of the Cu-ions on the membrane cell wall. This in turn allows for the translocation of Cu-ions into the bacteria cytoplasm, leading to cell lysis. Subsequently, this group showed the effect of sunlight on Cu grafted WO_3-TiO_2 powders, which increased the bacterial inactivation kinetics under light due the WO_3 interfacial charge transfer (IFCT) to TiO_2 [157]. The bacterial inactivation of bacteriophages and viruses on TiO_2/Cu was recently reported [158] by the same group on foam samples used in air cleaners. The results show that the pathogen count in the polluted air could be decreased using the approach suggested in this study, improving the performance with suitable TiO_2/Cu containing foams.

Physical vapor deposition (PVD) and chemical vapor deposition (CVD) have been widely used as mentioned in references [91–94] to coat glass, silicon, polymers, and steel with TiO_2 and other metals and metal/oxides. Work along these lines, coating TiO_2/Cu on silica by CVD at 500 °C has been reported [159]. Recently, the preparation of uniform, adhesive, robust antibacterial coatings of textiles and thin polymers such as polyethylene (PE), polyurethane (PU), and textiles resisting much lower temperatures up to 160 °C, has employed sputtering methods working below this temperature that is applied for short times, and has gained attention for the applications of 2D/3D sputtered materials in health facilities, garments, and many artifacts used in hospital facilities [23–26]. Pioneering work in this area has been carried out for two decades by P. Kelly, who has studied in a detailed and comprehensive way the sputtering configuration and the antibacterial performance of the sputtered surfaces. In conjunction with J. Veran, they have reported work that contributes to the understanding of the film microstructure and its effect on the abatement of pathogens [160–162].

Recently S. Pillai [163] has carried out work on the ability of TiO_2/Cu nanoparticulates co-doped with fluorine (F) to abate *Staphylococcus aureus* (MRSA) under visible light. Fluorine introduced visible light absorption in TiO_2, inducing Ti^{3+} and leading to O-vacancies and precluding e^-/h^+ recombination in TiO_2. A sol-gel preparation using aqueous titanyl acetate and titanyl trifluoroacetate with added Cu-nitrate was prepared according to US patent 9,210,934 [164]. The sol was then deposited on glass plates by dip-coating, and after drying was heated to 550 °C. In the initial anatase network, the O sites were substituted partially by F and the Ti by Cu [43,56]. The addition of F and Cu significantly improved the inactivation of MRSA under visible light irradiation, similar to that available in hospital facilities. When TiO_2 was doped only with F, the photocatalytic activity was observed to be below that registered for TiO_2/F/Cu, illustrating the synergistic effect of the combined doping of F and Cu. Cu-doping improved the bacterial inactivation on TiO_2, but TiO_2-F was ineffective for MRSA inactivation under dark conditions.

2.6. Current Work on TiO_2/Cu Sputtered Surfaces by DCMS, DCMSP, and HIPIMS, Bactericidal Effects and Thin Film Properties

In the sputtering chamber, the Cu- and Ti-targets shown in Figure 3 were bombarded by Ar-ions generated in the glow discharge plasma at a plasma working pressure was 0.4 Pa. The distance between the targets and the substrate was ~10 cm and the diameter of the 99.9% Cu and Ti targets was 5 cm. The deposition currents generally used for DCMS were 50–300 mA and a bias voltage of

100–300 V was applied. Under these conditions, the Cu and Ti-ions were estimated to penetrate up to about 20 nm on textile substrates [105–107,117].

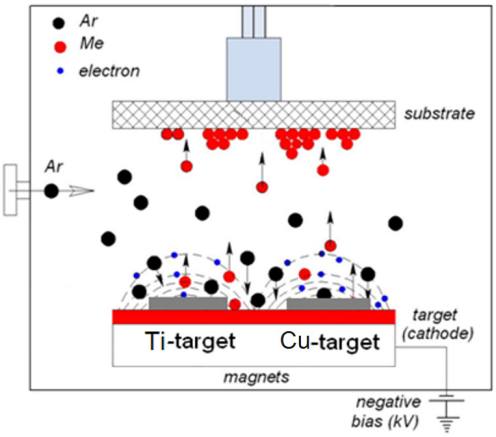

Figure 3. Schematic representation of the two target-sputtering unit used to deposit inactivating agents on the substrates.

The thin uniform TiO_2/Cu films on cotton, about 78 nm thick, were sputtered in the unit shown below. The most suitable films leading to bacterial inactivation consisted of Ti sputtered for 10 min, sequentially sputtered by Cu for 40 s at 300 mA, under a partial pressure of O_2 of 0.08 Pa and a partial pressure of Ar of 0.4 Pa. This Cu-doped sample inactivated *E. coli* within about 30 min in dark conditions.

Bacterial inactivation was completed within 5–6 min under low intensity actinic light >400 nm, providing evidence for: (a) the synergic interaction between Cu and TiO_2 and (b) the interfacial charge transfer (IFCT) occurring between TiO_2 and Cu under band-gap irradiation [165]. The bacterial inactivation involved redox catalysis. This is the variation of the Cu-oxidation state during the bacterial process due to the contact of the bacteria with the topmost Cu/CuO layers in the TiO_2/Cu sample. The evidence for this occurrence was obtained by X-ray photoelectron spectroscopy (XPS) for variations >0.2 ev in the spectrograms for Cu, O, and C observed for samples at time zero and for samples after the 5–6 min disinfection period induced under indoor visible light irradiation.

The diffuse reflectance spectra (DRS) of the sputtered TiO_2/Cu sample in Figure 4 shows that Cu does not substitute Ti^{4+} in the TiO_2 crystal lattice. Ti and Cu-ions were released in ppb amounts during bacterial disinfection, providing evidence that the bacterial inactivation involves predominantly an oligodynamic effect [76,118]. The small amounts of Cu released during disinfection electrostatically bind to the S– and N– and COO− negative groups of the bacterial cell wall before translocating onto the bacterial cytoplasm. This mechanism was originally suggested by the Tokyo University photocatalysis laboratory [155–158]. Figure 4 shows the Cu released during the disinfection cycles by a TiO_2/Cu (10 min/40 s) sputtered sample irradiated by actinic light (4 mW/cm^2). After each cycle, the samples were washed thoroughly before starting the next repetitive cycle. After the eighth cycle, Figure 4 shows Cu was released at ppb levels <8 ppb. These Cu-levels are not considered cytotoxic to mammalian cells [150,166].

Figure 5 shows a concomitant lower release of 8 ppb Ti-ions during bacterial disinfection, which dropped to about 4 ppb after the eighth cycle. This lower Ti-ion release is consistent with the very high stability reported for TiO_2 up to pH ~ 13.

TiO_2/Cu cotton samples increased the *E. coli* inactivation kinetics with the increase of the applied light intensity [166]. Therefore, the predominant effect leading to bacterial inactivation seems to be due to the photo-generated charges either by: (a) the TiO_2; (b) the intermetallic TiO_2/Cu and TiO_2-Cu phases; and finally (c) the CuO.

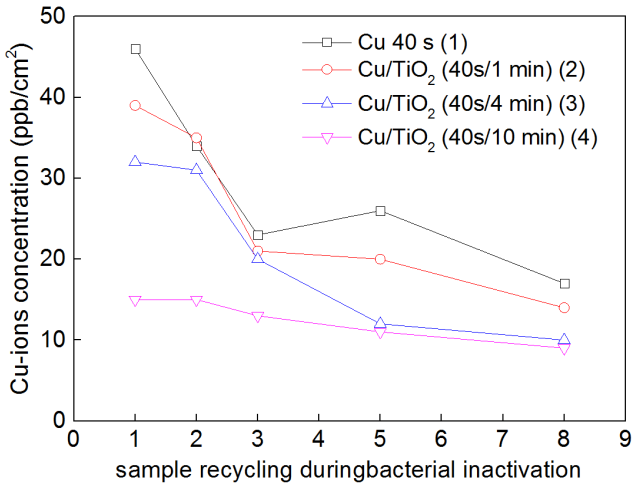

Figure 4. Cu ions release from diverse Cu-cotton and TiO_2/Cu-cotton sputtered films as a function of catalyst cycling up to the 8th cycle.

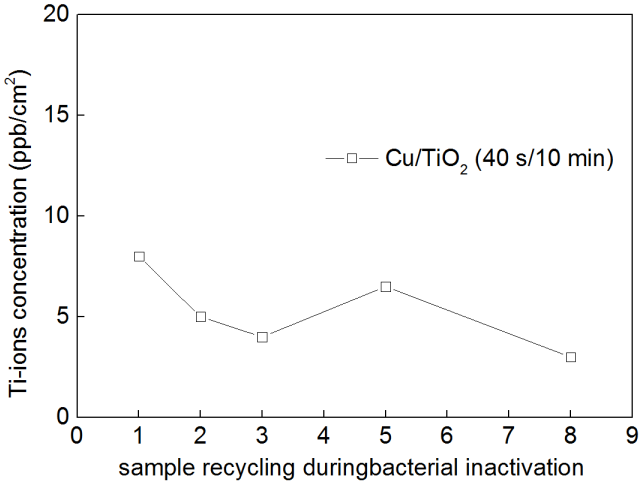

Figure 5. Ti-ions release from a diverse TiO_2/Cu (10 min/40 s) cotton sputtered sample as a function of catalyst cycling up to the eighth cycle.

2.7. TiO_2-Cu Films by HIPIMS: Comparison of the Bacterial Inactivation Performance with DCMS/DCMSP-Films

In a recent study, we reported that sputtering by HIPIMS on polyester (PES) showed that thinner TiO_2-Cu HIPIMS sputtered films (~40 nm) induced bacterial inactivation of *E. coli* within 9–12 min compared to bacterial inactivation on thicker TiO_2/Cu sequentially sputtered by DCMS/DCMSP (600 nm thick) [125]. To carry out the HIPIMS co-sputtering, the target used was 60%Ti/40%Cu by weight and the pulse used 5 A and 350 V with a power of 1750 W during the 100 microsecond pulses. DCMS of TiO_2 (0.3 A) was followed by Cu-sputtering by DCMSP (0.3 A/622 V) with pulses of 10 microseconds at an average power of 187 W/pulse. Figure 6 presents the loss of viability kinetics vs. thickness for the DCMS/DCMSP and HIPIMS TiO_2-Cu sputtered films. Figure 6 shows that the much thinner TiO_2-Cu layer sputtered by HIPIMS was required for complete bacterial inactivation, compared to that by DCMS/DCMSP.

Coated polyester (PES) films sputtered by DCMS/DCMSP in Figure 6 proceeded at much lower energies compared to HIPIMS films. DCMS prepared TiO_2/Cu films in Figure 6 induced bacterial inactivation by films ~15 times thicker compared to the HIPIMS prepared films [107,108]. In Figure 6, the HIPIMS films have the following characteristics: 40 nm thickness, 5 ± 2 nm size of the TiO_2/Cu

nanoparticles, and the TiO_2 anatase phase as determined by XRD. The DCMS/DCMSP films presented a thickness of 600 nm, 20 ± 5 nm Cu/TiO_2 nanoparticles, and the TiO_2 anatase phase was also found.

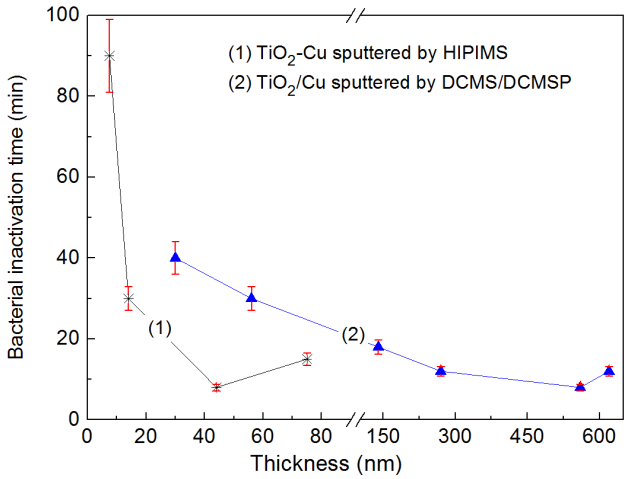

Figure 6. Bacterial inactivation time vs. nominal thicknesses for TiO_2/Cu sputtered by High Power Impulse Magnetron Sputtering (HIPIMS) films and TiO_2/Cu sputtered by Direct Current Magnetron Sputtering or Pulsed Direct Current Magnetron Sputtering (DCMS/DCMSP) irradiated under Osram Lumilux 18 W/827 actinic lamp (4 mW/cm^2). Error bars: standard deviation (n = 10%).

In the seminal work cited in reference [107], Figure 7 shows that the optimized Cu/TiO_2 coating inactivates bacteria within 10 min. The bacterial inactivation depends on the film thickness in the following way: concomitant to the variation of the film thickness (increase or decrease), the roughness of the layers will also vary, presenting different values for the average roughness R_a. A higher roughness shows the existence of peaks more closely packed on the substrate surface. An optimal value for the roughness is not necessarily related to thicker coatings but is a function of many surface properties developed on the sputtered layers. This is why the roughness has to be determined for each individual coating, generally by AFM, for metal/oxides or composite microstructures.

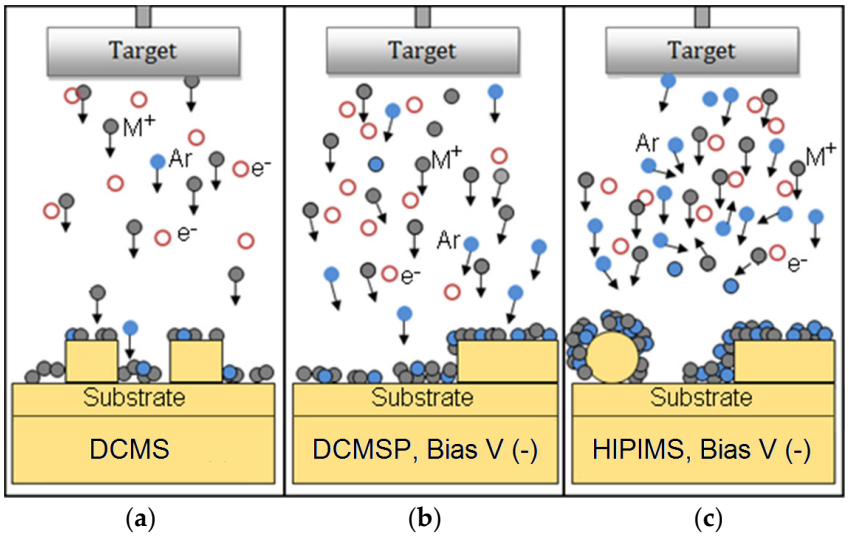

Figure 7. Schematics of the (**a**) DCMS, (**b**) DCMSP and (**c**) HIPIMS sputtering of metal-ions (M^+) on 3-D surfaces.

In Figure 7, the left-hand side presents a scheme for the DCMS sputtering proceeding with a low ionization of the Cu-ions of ~1%–5% [126]. The DCMSP of Cu is shown in the middle section of Figure 7, attaining Cu-ionization of 5%–10% with an electronic density of ~10^{15-16} e^-/m^3 [107,108,120]. This is well above the Cu-ionization percentages attained by DCMS [107,120–122,125,126]. In the case of the DCMS/DCMSP Cu/TiO_2 films, the fastest bacterial inactivation was attained by sputtering TiO_2 by DCMS for 10 min followed by Cu-DCMSP for 60 s. The right-hand section of Figure 7 shows the density of the species attained by HIPIMS that is able to ionize Cu up to 70% with an electronic density in the plasma of ~10^{18-19} e^-/m^3 [101]. HIPIMS sputtering for 150 s, applying a current of 5 A on a mixed target Cu/TiO_2 (60% TiO_2 and 40% Cu), led to a film with a composition of 0.08% CuO and 0.44% TiO_2 by weight. The higher energy HIPIMS increases the amount of ionized Cu-ions in the reaction:

$$Cu^0 \rightarrow Cu^+/Cu^{2+} \quad (24)$$

Cu^0 in Equation (24) refers to Cu-metal.

HIPIMS sputtered TiO_2 for 10 min and Cu for 60 s on PES inactivated *E. coli* under actinic light as shown in Figure 6. Figure 8 shows the release of Cu-ions that are inactivating *E. coli* from the HIPIMS sputtered TiO_2-Cu PES as a function of catalyst recycling. Inductively coupled plasma spectrometry (ICP-MS) was used to determine the Cu, since it is a sensitive analytical technique. A Finnigan™ ICPS was used and was equipped with a double focusing reverse geometry mass spectrometer with a resolution of 1.2 × 10^5 cps/ppb, and a detection limit of 0.2 ng/L. Samples 1 cm^2 were placed in Eppendorf tubes containing a 1 mL solution (NaCl/KCl). The solutions were then diluted 10 times to reach the volume and/or dilution necessary for the ICP-MS analyses. After the eighth recycling, the release of Cu was ~8 ppb/cm^2. This value is lower than the Cu release from the Cu-sputtered PES samples of ~18 ppb Cu/cm^2 after the eighth cycle. This shows the stabilizing/protective/adhesive effect of TiO_2 on the Cu. Release of Cu at the ppb levels shown in Figure 8 are not considered to be cytotoxic to mammalian cells. The *E. coli* disinfection cycles shown in Figure 8 may well proceed through an oligodynamic effect. This toxic effect of metals such as Cu at extremely low concentrations leads to the inactivation of bacteria, fungi, and viruses [76,118,150]. Please make sure that the intended meaning is retained.

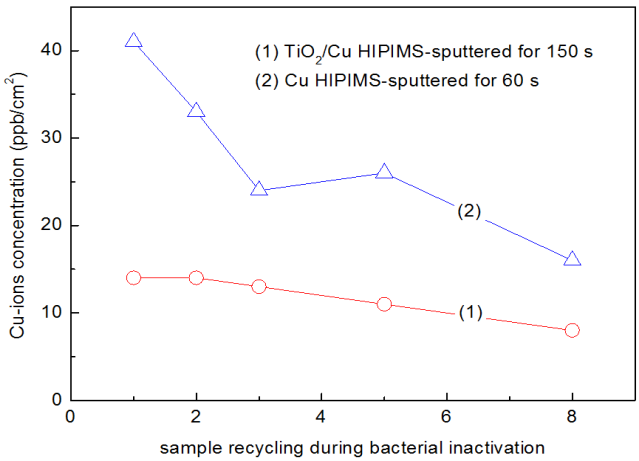

Figure 8. The concentration of ions eluted into solution determined by Inductively Coupled Plasma Mass Spectrometry (ICP-MS) up to the eighth recycling of TiO_2/Cu prepared by High Power Impulse Magnetron Sputtering (HIPIMS) sputtered samples, inactivating *E. coli* under actinic light.

HIPIMS sputtered for 30 s show Cu nanoparticles between 8 and 15 nm. The TiO_2 samples sputtered for 150 s present sizes between 8 and 12 nm, and the TiO_2-Cu samples sputtered for 150 s presented particles 5–10 nm. TiO_2 has been suggested to bind, disperse, and stabilize the Cu-clusters on the PES surfaces. The distribution of TiO_2 and Cu nanoparticles on the PES in Figure 9 was found

to be uniform, with no cracks present. Figure 10a presents the contrasted high angular annular dark field (HAADF) TiO_2/Cu microscopy image, showing the Cu nanoparticles to be immiscible with Ti. Figure 10b shows the mapping/distribution of the Cu, Ti, and O on PES.

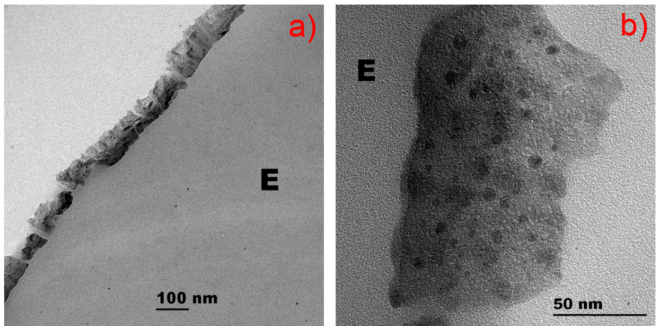

Figure 9. Transmission electron microscopy (TEM) of: (**a**) Cu sputtered for 150 s by HIPIMS on polyester; (**b**) Cu-TiO_2 sputtered for 150 s by HIPIMS on polyester.

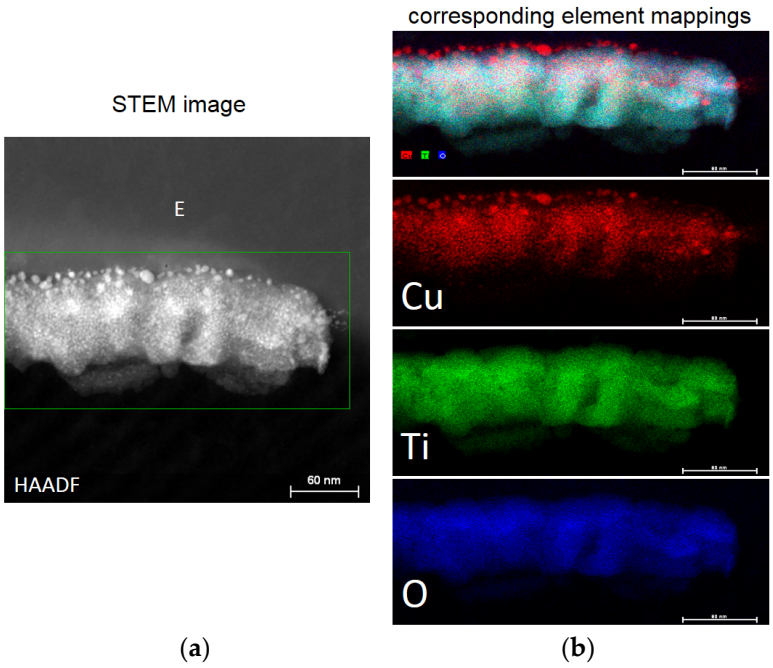

Figure 10. (**a**) High-Angle Annular Dark-Field imaging (HAADF) images of Cu-TiO_2 HIPIMS sputtered for 150 s showing the complete sample and (**b**) the mapping of Cu, Ti, and O by Z-contrast imaging.

Transmission electron microscopy was carried out in a FEI Tecnai TEM-STEM Osiris (200 kV, EDX: FEI Super-X; software: Esprit analysis, Bruker Nano), and was used to measure the grain size of the TiO_2/Cu films. To carry out this observation, textiles were embedded in epoxy resin 45359 Fluka (designated as E in Figures 9 and 10) and the fabrics were cross-sectioned with an ultramicrotome at a knife angle of 35°. These images (Z-contrast images) were obtained by collecting the scattered electrons passing through the objective provided with an annular dark-field detector.

Due to the small size found for the CuO/Cu nanoparticles as reported in Figure 9, these CuO/Cu nanoparticles are not able to penetrate into the bacteria core through the cell wall porins with diameters of 1–1.3 nm [109]. However, Cu-ions are able to diffuse through the cell wall porins leading to cytoplasm/DNA damage and finally to the loss of bacterial viability.

2.8. Interfacial Charge Transfer (IFCT) Suggested on TiO_2-Cu Films Leading to Gram-Negative and Gram-Positive Bacterial Inactivation

Figure 11 shows the interfacial charge transfer between TiO_2 and Cu under simulated solar irradiation. In the TiO_2 semiconductor, the irradiation with solar simulated light in the cavity of the solar simulator has been suggested to transfer e^- and h^+ from TiO_2 to CuO. Charge transfer from ad-atoms to TiO_2 under light has been investigated for the last three decades [167]. The potential energy levels of the TiO_2cb and TiO_2vb lie above the CuOcb and CuOvb levels, as shown in Figure 11. The partial recombination of e^-/h^+ in TiO_2 would be hindered by the charge injection into CuO. The interfacial charge transfer (IFCT) to TiO_2 from the CuOvb at +1.4 eV to the TiO_2vb at +2.5 eV vs. SCE, pH 0, proceeds with considerable driving force due to the large difference between these two vb levels. This model for the charge transfer between TiO_2 and CuO under solar light (UV-Vis) has been suggested by Hashimoto [107,156,168] and is presented in Figure 5. The *E. coli* inactivation times proceeding within 10 min is shown in Figure 11. These TiO_2vb holes react with the surface –OH groups of the TiO_2 releasing OH-radicals. The CuO nanoparticles on the TiO_2 can be reduced to Cu_2O by the charges generated in the TiO_2 under light and can later re-oxidize to CuO, as shown in Figure 11.

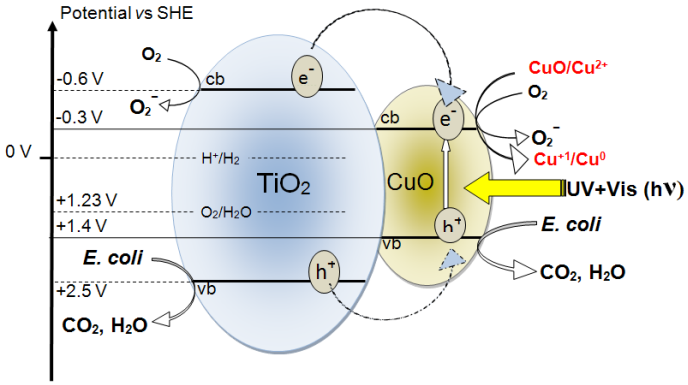

Figure 11. Scheme of bacteria inactivation under light on Cu-TiO_2 films on polyester.

The electronic transfer between the TiO_2/Cu and *E. coli* depends on the length of the charge diffusion in the TiO_2/Cu. The diffusion is a function of the TiO_2 and Cu particle size and shape [101,121]. The interfacial distances between TiO_2 and Cu/CuO on the polyester surface ranges from 5 nm and up. The IFCT, as shown in Figure 5, proceeds with high quantum efficiency depending on the applied light intensity and the nanoparticulate size and surface properties [155–158]. Quantum size effects occur in particles with sizes ~10 nm that have about 10^4 atoms (Figure 9) [122]. The surface composition and properties of the TiO_2-CuO play a role in the charge transfer kinetics involving: (a) surface defects; (b) surface imperfections; and (c) dangling bonds on the edge of this composite. Using XPS and atomic force microscopy (AFM), information on the surface composition and roughness has been partially reported [169]. In TiO_2-Cu the charge recombination is short due to their small particle size. The small particle size decreases the space for charge separation. Also, the semiconductor space charge layer in both the TiO_2 and CuO further decreases the potential depth available for the charge injection at the TiO_2-Cu heterojunction. This decreases the energy difference between TiO_2 and Cu, which is not favorable for the charge injection [43,56,107]. The conduction band of CuO at −0.30 V vs. SCE (pH 7) in Figure 5 is at a more negative potential than the potential required for one electron oxygen reduction [125,155–158]. Furthermore, the Cu^{2+} can also react with O_2^-

$$O_2 + H^+ + e^- \rightarrow HO_2^\bullet \; -0.22 \text{ V} \quad (25)$$

$$Cu^{2+} + O_2^- \rightarrow Cu^+ + O_2 \quad (26)$$

A recent study addressed the inactivation of *E. coli* and MRSA on co-sputtered TiO_2-Cu to compare the PES sputtered samples in the dark and under light on Gram-negative and Gram-positive bacteria [170]. The TiO_2-Cu-PES was obtained by direct current magnetron co-sputtering for 3 min and induced Gram-negative *E. coli* inactivation within 120 min in the dark within 30 min under low intensity actinic light. The inactivation of MRSA (with an intial concentration of 10^6 CFU/mL) on co-sputtered TiO_2-Cu attained 99.99% within 120 min in the dark and within 30 min under indoor actinic light irradiation, as shown in Figure 6a. Cu was released in ppb amounts during the bacterial inactivation as detected by inductively coupled plasma-mass spectrometry (ICP-MS), suggesting an oligodynamic effect.

Figure 12 trace 1 shows bacterial inactivation within 30 min for TiO_2-Cu co-sputtered for 3 min. This film was determined by profilometry to be 135 nm thick (about 700 atomic layers) consisting of 0.16% Cu weight/TiO_2 0.14% by weight on PES as determined by X-ray fluorescence (XRF) on the PES substrate [169]. This coating provides a sufficient amount of TiO_2 and Cu on the PES to interact meaningfully with bacteria. Co-sputtering for 1 and 2 min did not induce the necessary amount of TiO_2 and Cu-sites, leading to an accelerated bacterial inactivation.

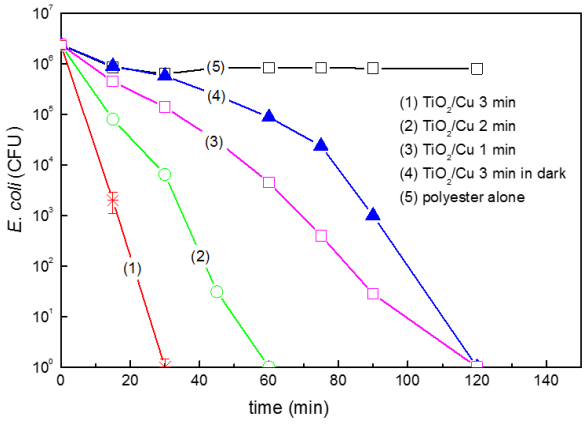

Figure 12. *E. coli* inactivation on TiO_2-Cu co-sputtered for different times on polyester (PES) as indicated in the traces: (1) 3 min, (2) 2 min, (3) 1 min, (4) co-sputtered TiO_2-Cu for 3 min in the dark and (5) PES-alone. The bacterial reduction under light irradiation used a Philips Master-18W/865 lamp (4.65 mW/cm^2).

Next, we address the issue of the MRSA bacterial inactivation kinetics and relate the inactivation time to the applied light intensity. A longer inactivation time was observed for MRSA compared to *E. coli* under light irradiation. This is shown in Figures 12 and 13. The difference in wall thickness, number of layers, peptidoglycan content, lipid and protein content, and lipopolysaccharide (LPS) content seems to account for the different bacterial inactivation kinetics observed for *E. coli* and MRSA [6–9,13,64,136]. The electrostatic interaction of the Cu NPs-positive-ions interacting with the negative lipopolysaccharide (LPS) of *E. coli* will certainly be different to the interaction of the Cu-NPs ions interacting with the positive outer layer of MRSA. Figure 13a shows the MRSA inactivation time in the dark under different conditions and for different MRSA loadings. Next, Figure 13b shows MRSA inactivation under three different light intensities. The MRSA inactivation in the dark and under actinic light irradiation occurred within similar times, suggesting an inactivation mechanism completely different to the one leading to the inactivation of *E. coli* (Figure 12). Some studies have recently appeared in the literature about the inactivation of Gram-negative and Gram-positive bacteria on Cu-composites [171,172].

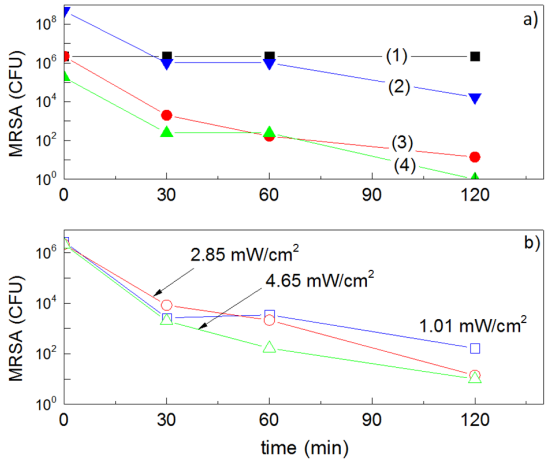

Figure 13. (**a**) Effect of the initial bacterial concentration of MRSA loss of viability on: (1) Unsputtered PES and by co-sputtered TiO_2/Cu-PES for 3 min tested in the dark: (2) 10^8 CFU/mL, (3) 10^6 CFU/mL and (4) 10^5 CFU/mL. (**b**) Effect of light intensity on MRSA loss of viability on co-sputtered TiO_2/Cu-PES for 3 min under: 1.01, 2.85, and 4.65 mW/cm^2.

During the last two years, some studies reported the sputtering of binary oxide Cu promoted films. Reports on their bacterial inactivation kinetics, adhesion, and mechanical strength seem encouraging at this stage. The long-term operational lifetime and inactivation mechanism have been reported alongside the amount of Cu released by these innovative surfaces during bacterial inactivation. These studies have shown a drastic enhancement of the bacterial inactivation kinetics of *E. coli* when Cu was added to binary-oxides in percentages from 0.01% (decoration) up to 1% (doping) [119,127,173]. A variety of TiO_2-Cu preparations and the evaluation of their activity for diverse applications is an area of current interest [129–131,174].

The relevance of TiO_2-Cu catalysts and photocatalysts addressing the issue of bacterial inactivation is reflected in the increasing number of studies focusing on the antibacterial effects of TiO_2-Cu and TiO_2/Cu in the form of 2D-coatings, suspensions, spheres, alloys, and decorated binary oxides [175–181].

In Section 2.1, Equations (5)–(9) presented a scheme of reactions leading to bacterial inactivation by TiO_2 sputtered on PE. A recent study presents evidence for binary TiO_2-ZrO_2 sputtered on PES behaving in a similar way to TiO_2, but leading to shorter times of bacterial inactivation under band-gap irradiation [172]. Only ppb amounts decorating the surface of TiO_2-ZrO_2 and TiO_2 were shown to be necessary to drastically accelerate bacterial reduction. The minimal amounts of Cu as determined by XRF were in the range of 0.01%–0.02% by weight (ppb range). The drastic effect of extremely low amounts of Cu released during the bacterial inactivation can be rationalized by the high toxicity of Cu(Cu(I)/Cu(II) species/oxides on the bacteria and cannot be ascribed to any doping of the TiO_2 by Cu, which requires much higher Cu-amounts. Recent developments on flexible antibacterial sputtered coatings have been reported using Cu as a bactericide agent in the composite films [182–184].

3. Conclusions

The Cu and TiO_2 semiconductors interact with the bacterial wall and the cytoplasm in the dark and under light conditions by mechanisms that remain controversial. This review focused on uniform, stable, and reproducible Cu/TiO_2 or Cu-TiO_2 films obtained by sequential sputtering or by co-sputtering. Accelerated bacterial inactivation kinetics were observed by the co-sputtered films compared to the sequentially sputtered films in the dark or under indoor visible light irradiation. The evaluation of the bacterial inactivation kinetics, the disinfection stability, and last but not least, the properties of the sputtered films leading to the bacterial inactivation were addressed in detail.

Considerable savings in metal and deposition time (energy) was found by using HIPIMS sputtering compared to conventional DCMS/DCMSP sputtering. This is important due to the increasing demand for Cu, which is rapidly decreasing the known Cu reserves in the world. It seems that the biocide properties of Cu drastically increase the bactericidal properties of TiO_2. Progress in the knowledge of the molecular mechanism implicated in the bacteria-TiO_2/Cu is needed to design and synthesize more effective antibacterial biomaterial-composites. This is an important point in view of the current limitations of the use of antibiotics over long time periods and the increasing resistance of many toxic pathogens to antibiotic/antiseptic formulations. The photocatalysis mediated by TiO_2, Cu, and Cu/TiO_2 under light and for Cu-containing surfaces in the dark led to bacterial inactivation for *E. coli* and MRSA. The oxidative intermediate radicals generated during the photocatalysis degrade/mineralize both types of bacteria independently of the specific bacterial charge.

Acknowledgments: The authors thank the support by the EPFL and the financial support by the Swiss National Science Foundation under Grant No 2000021-143283/1.

Author Contributions: S.R. carried out the sputtering of the Cu/TiO_2 and TiO_2-Cu films, their characterization, and biological evaluation. C.P. contributed with his microbiological and catalytic/photocatalytic experience to the studies presented in this review. J.K. participated in the overall work leading to this review and coordinated the layout of the final write-up with S.R. The authors gave their final approval for the submitted manuscript and are accountable for the material presented in this review.

Conflicts of Interest: The authors declare no conflict of interest.

References

1. Mikolay, A.; Hugget, S.; Tikana, L.; Grass, G.; Braun, J.; Nies, D. Survival of bacteria on metallic copper surfaces in a hospital trial. *Appl. Microbiol. Biotechnol.* **2010**, *87*, 1875–1879. [CrossRef] [PubMed]
2. Sunada, K.; Watanabe, T.; Hashimoto, K. Bactericidal activity of copper-deposited TiO_2 films under weak UV-light illumination. *Environ. Sci. Technol.* **2003**, *37*, 4785–4789. [CrossRef] [PubMed]
3. Nozik, A. Photo-electrochemistry: Applications to Solar Energy Conversion. *Annu. Rev. Phys. Chem.* **1978**, *189*, 521–549.
4. Yadava, H.; Otaria, S.; Kolia, V.; Malib, S.; Hong, C.; Pawara, S.; Delekara, S. Preparation and characterization of copper-doped anatase TiO_2 nanoparticles with visible light photocatalytic antibacterial activity. *J. Photochem. Photobiol. A Chem.* **2014**, *280*, 32–38. [CrossRef]
5. Rtimi, S.; Giannakis, S.; Bensimon, M.; Pulgarin, C.; Sanjines, R.; Kiwi, J. Supported TiO_2 films deposited at different energies: Implications of the surface compactness on the catalytic kinetics. *Appl. Catal. B* **2016**, *191*, 42–52. [CrossRef]
6. Robin, S.; Soulimane, T.; Lavelle, S. Interactions of Biofilm-forming Bacteria with Abiotic Surfaces. In *Biological Interactions with Surface Charges in Biomaterials*; Tofail, S.A.M., Ed.; RSC: London, UK, 2012.
7. Lejeune, P. Contamination of abiotic surfaces: What a colonizing bacterium sees and how blur it. *Trends Microbiol.* **2003**, *11*, 179–184. [CrossRef]
8. Bernstein, R.; Freger, V.; Lee, J.; Kim, Y.; Lee, J.; Herzberg, M. Should I stay or should I go? Bacterial attachment vs. biofilm formation on surface-modified membranes. *Biofouling* **2014**, *30*, 367–376. [CrossRef] [PubMed]
9. Francolini, I.; Norris, P.; Piozzi, A.; Donello, G.; Stoodley, P. Usnic acid, a natural antimicrobial agent able to inhibit bacterial biofilm formation on polymer surfaces. *Antimicrob. Agents Chemother.* **2001**, *48*, 4360–4365. [CrossRef] [PubMed]
10. Francolini, I.; Donelli, G. Prevention and control of biofilm-based medical device-related infections. *FEMS Immunol. Med. Microbiol.* **2010**, *59*, 227–238. [CrossRef] [PubMed]
11. Hoiby, N.; Bjarnsholt, T.; Givskov, M.; Molin, S.; Ciofu, O. Antibiotic resistance of bacterial biofilms. *Int. J. Antimicrob. Agents* **2010**, *35*, 322–332. [CrossRef] [PubMed]
12. Byrne, A.-J.; Dunlop, M.S.P.; Hamilton, J.W.J.; Fernandez-Ibanes, P.; Polo-Lopez, I.; Sharma, K.P.; Vennard, M.S.A. A review of heterogeneous photocatalysis for water and surface disinfection. *Molecules* **2015**, *20*, 5574–5615. [CrossRef] [PubMed]
13. Canpoccia, D.; Montanaro, L.; Arciola, C. A review of the biomaterials technologies for infection resistant surfaces. *Biomaterials* **2013**, *34*, 8533–8554. [CrossRef] [PubMed]

14. Sun, D.; Shahzad, B.; Li, M.; Wang, G.; Xu, D. Antimicrobial materials with medical applications. *Mater. Technol. Adv. Biomater.* **2015**, *30*, B30–B95. [CrossRef]
15. Klevens, R.M.; Edwards, J.R.; Richards, C.L., Jr.; Horan, T.C.; Gaynes, R.P.; Pollock, D.A.; Cardo, D.M. Estimating health care-associated infections and deaths in U.S. hospitals, 2002. *Public Health Rep.* **2007**, *122*, 160–166. [CrossRef] [PubMed]
16. Zarb, P.; Coignard, B.; Griskeviciene, J.; Muller, A.; Vankerckhoven, V.; Weist, K.; Goossens, M.; Vaerenberg, S.; Hopkins, S.; Catry, B.; et al. The European Centre for Disease Prevention and Control (ECDC) pilot point prevalence survey of healthcare-associated infections and antimicrobial use. *Euro Surveill.* **2012**, *17*, 20316. [PubMed]
17. Boucher, H.W.; Talbot, G.H.; Bradley, J.S.; Edwards, J.E.; Gilbert, D.; Rice, L.B.; Scheld, M.; Spellberg, B.; Bartlett, J. Bad bugs, no drugs: No ESKAPE! An update from the Clinical infectious diseases Infectious. *Dis. Soc. Am.* **2009**, *48*, 1–12.
18. Bhalla, A.M.D.; Pultz, N.J.B.S.; Gries, D.M.M.D.; Ray, A.J.M.D.; Eckstein, E.C.R.N.; David, C.; Aron, M.D.; Donskey, C.J.M.D. Acquisition of Nosocomial Pathogens on Hands after Contact With Environmental Surfaces Near Hospitalized Patients. *Infect. Control Hosp. Epidemiol.* **2004**, *25*, 164–167. [CrossRef] [PubMed]
19. French, G.L.; Otter, J.A.; Shannon, K.P.; Adams, N.M.; Watling, D.; Parks, M.J. Tackling contamination of the hospital environment by methicillin-resistant *Staphylococcus aureus* (MRSA): A comparison between conventional terminal cleaning and hydrogen peroxide vapour decontamination. *J. Hosp. Infect.* **2004**, *57*, 31–37. [CrossRef] [PubMed]
20. Abreu, A.C.; Tavares, R.R.; Borges, A.; Mergulhao, F.; Simoes, M. Current and emergent strategies for disinfection of hospital environments. *J. Antimicrob. Chemother.* **2013**, *68*, 2718–2732. [CrossRef] [PubMed]
21. Matsunaga, T.; Tomoda, R.; Nakajima, T.; Nakamura, N.; Komine, T. Continuous-Sterilization System that Uses Photosemiconductor Powders. *Appl. Environ. Microbiol.* **1988**, *54*, 1330–1333. [PubMed]
22. Fujishima, A.; Hashimoto, K.; Watanabe, W. *TiO_2 Photocatalysis Fundamentals and Applications*; Bkc Inc.: Tokyo, Japan, 1999.
23. Taylor, K.; Roberts, J.; Roberts, J. *The Challenge of Hospital Acquired Infections (HAI)*; National Audit Office: London, UK, 2002.
24. Talon, D. The role of the hospital environment in the epidemiology of multi-resistant bacteria. *J. Hosp. Infect.* **1999**, *43*, 13–17. [CrossRef] [PubMed]
25. Kramer, A.; Schwebke, I.; Kampf, G. How long do nosocomial pathogens persist on inanimate surfaces? A systematic review. *BMC Infect. Dis.* **2006**, *6*, 130–139. [CrossRef] [PubMed]
26. Dancer, S.J. The role of environmental cleaning in the control of hospital-acquired infection. *J. Hosp. Infect.* **2009**, *73*, 378–385. [CrossRef] [PubMed]
27. Pakrashi, S.; Kumar, R.; Chandrasekaran, N.; Mujerkee, A. A comparative cytotoxicity study of TiO_2 nanoparticles under light and dark conditions at low light exposure concentrations. *Toxicol. Res.* **2012**, *1*, 116–130.
28. Zhang, L.; Luo, Z.; Song, L.; Shi, X.; Pan, Y.; Fan, Y.; Xu, Y. Effects and mechanisms of waterborne copper exposure influencing ovary development and related hormones secretion in yellow catfish Pelteobagrus fulvidraco. *Aquat. Toxicol.* **2016**, *178*, 88–98. [CrossRef] [PubMed]
29. Anderl, J.; Franklin, M.; Stewart, R. Role of antibiotic penetration limitation in *Klebsiella pneumoniae* biofilm resistance to ampicillin and ciprofloxacin. *J. Antomicrob. Agents Chemother.* **2000**, *44*, 1818–1824. [CrossRef]
30. Matsunaga, T.; Tomoda, R.; Nakajima, T.; Wake, H. Photoelectrochemcal sterilization of microbial cells by semiconductor powders. *FEMS Microb. Lett.* **1985**, *29*, 211–214. [CrossRef]
31. Foster, H.; Ditta, I.; Varghese, S.; Steele, A. Photocatlytic disinfection using titanium dioxide: Spectrum and mechanism of antimicrobial activity. *Appl. Microbiol. Biotechnol.* **2011**, *90*, 1847–1868. [CrossRef] [PubMed]
32. Pigeot-Rémy, S.; Simonet, F.; Errazuriz-Cerda, E.; Lazzaroni, J.; Atlan, D.; Gillard, C. Photocatalysis and disinfection of water: Identification of potential bacterial targets. *Appl. Catal. B* **2011**, *104*, 390–398. [CrossRef]
33. Markowska-Szczupak, A.; Ulgig, K.; Morawski, A. The applicationot titanium dioxide for deactivation of bioparticulates: An overview. *Catal. Today* **2011**, *169*, 249–257. [CrossRef]
34. Robertson, P.; Robertson, J.; Bahnemann, D. Removal of microorganisms and their chemical metabolites from water using semiconductors photocaatlysis. *J. Hazard. Mater.* **2012**, *211–212*, 162–171.
35. Dalrymple, O.; Isaaks, W.; Stefanakos, E.; Trotz, M.; Goswami, D. Lipid vesicles a smodel membranes in photocatalytic disinfection studies. *J. Photochem. Photobiol. A* **2011**, *221*, 64–70. [CrossRef]

36. Gamage, J.; Zhang, Z. Applications of Photocatalytic Disinfection: A review. *Int. J. Photo-Energy* **2010**, *2010*, 764870. [CrossRef]
37. Kubacka, A.; Diez, M.S.; Rojo, D.; Bargiela, R.; Ciordia, S.; Zapico, I.; Albar, J.P.; Barbas, C.; Martins dos Santos, V.A.P.; Fernández-García, M.; et al. Understanding the antimicrobial mechanism of TiO_2-based nanocomposite films in a pathogenic bacterium. *Sci. Rep.* **2014**, *4*, 4134–4143. [CrossRef] [PubMed]
38. Dalrymple, O.; Stefanakos, E.; Trotz, M.; Goswami, Y. A review of the mechanism and modeling of photocatalytic disinfection. *Appl. Catal. B* **2010**, *98*, 27–38. [CrossRef]
39. Farr, S.; Kogoma, T. Oxidative stress responses in *Escherrichia coli* and *Salmonella triphimurium*. *Microbiol. Rev.* **1991**, *55*, 561–585. [PubMed]
40. Kiwi, J.; Nadtochenko, V. New evidence for TiO_2 photocatalysis during bilayer lipid-peroxidation. *J. Phys. Chem. B* **2004**, *108*, 17675–17684. [CrossRef]
41. Linsebliger, A.; Lu, G.; Yates, J. Photocatalysis on TiO_2 Surfaces. Principles, Mechanisms and Selected Results. *Chem. Rev.* **1996**, *95*, 735–758. [CrossRef]
42. Nakano, R.; Hara, M.; Ishiguro, H.; Yao, Y.; Ochiai, T.; Nakata, K.; Murakami, T.; Kajioka, J.; Sunada, K.; Hashimoto, K.; et al. Broad Spectrum Microbicidal Activity of Photocatalyis by TiO_2. *Catalysts* **2013**, *3*, 310–323. [CrossRef]
43. Fujishima, A.; Zhang, X.; Tryk, D. TiO_2 photocatalysis and related surface phenomena. *Surf. Sci. Rep.* **2008**, *63*, 515–582. [CrossRef]
44. Daoud, W. *Self-Cleaning Materials and Surfaces, a Nanotechnology Approach*; Wiley: Chichester, UK, 2013.
45. Griesser, H.J. Chapter 16: Uniform, adhesive and low cytotoxic films accelerating bacterial reduction in the dark and under visible light. In *The Film Coatings for Biomaterials and Biomedical Applications*; Rtimi, S., Pulgarin, C., Kiwi, J., Eds.; Elsevier Ltd.: London, UK, 2016.
46. Kiwi, J.; Rtimi, S. Chapter 3: Environmentally mild self-cleaning processes on textile surfaces under daylight irradiation: Critical Issues. In *Active Coatings for Smart Textiles*; Hu, J., Ed.; Elsevier Ltd.: Cambridge, UK, 2016.
47. Rtimi, S.; Sanjines, R.; Kiwi, J.; Pulgarin, C.; Bensimon, M.; Khmel, I.; Nadtochenko, V. Innovative photocatalysts (FeO_x-TiO_2): Transients by femtosecond laser pulse leading to bacterial inactivation under visible light. *RSC Adv.* **2015**, *5*, 101751–101759. [CrossRef]
48. Rtimi, S.; Pulgarin, C.; Nadtochenko, V.; Gostev, F.; Shelaev, I.; Kiwi, J. FeO_x-TiO_2 Film with Different Microstructiures Leading to Femtosecond Transients with Different Properties: Biological Implications under Visible Light. *Nat. Sci. Rep.* **2016**, *6*, 30113. [CrossRef] [PubMed]
49. Pelaez, M.; Nolan, T.; Pillai, C.S.; Seery, K.; Falaras, P.; Kontos, A.; Dunlop, M.; Dunlop, H.J.; Byrne, A.-J.; O'Shea, K.; et al. A review on the visible light active titanium dioxide photocatalysts for environmental applications. *Appl. Catal. B* **2012**, *125*, 331–349. [CrossRef]
50. Banerjee, S.; Pillai, C.S.; Falaras, P.; O'Shea, K.; Byrne, A.-J.; Dionysiou, D. New Insights into the Mechanism of Visible Light Photocatalysis. *J. Phys. Chem. Lett.* **2014**, *5*, 2543–2554. [CrossRef] [PubMed]
51. Etacheri, V.; Di Valentin, C.; Schneider, D.; Bahnemann, D.; Pillai, C.S. Visible-light activation of TiO_2 photocatalysts: Advances in theory and experiments. *J. Photochem. Photobiol. C Rev.* **2015**, *25*, 1–29. [CrossRef]
52. Banerjee, S.; Dionysiou, D.; Pillai, C.S. Self-cleaning applications of TiO_2 by photo-induced hydrophilicity and photocatalysis. *Appl. Catal. B* **2015**, *176–177*, 396–428. [CrossRef]
53. Fagan, R.; Cormack, M.; Dionysiou, D.; Pillai, S. A review on solar and visible light active TiO_2 photocatalysts for treating bacteria, cynotoxins and contaminants of emerging concern. *Mater. Sci. Semicond. Process.* **2016**, *42*, 2–14. [CrossRef]
54. Devi, G.; Kavitha, R. A review on non-metal ion doped-titania for photocatalytic degradation of organic pollutants under UV/solar light: Role of photogenerated charges dynamic in enhancing the activity. *Appl. Catal. B* **2013**, *140–168*, 559–587. [CrossRef]
55. Fotiou, T.; Triantis, T.; Kaloudis, T.; O'Shea, K.; Dionysiou, D.; Hiskia, A. Assessment of the roles of reactive oxygen species in the UV and visible light photocatalytic degradation of cyanotoxins and water taste and odor compounds using C-TiO_2. *Water Res.* **2016**, *90*, 52–61. [CrossRef] [PubMed]
56. Schneider, J.; Matsuoka, M.; Takeuchi, J.; Zhang, L.; Horiuchi, Y.; Anpo, M.; Bahnemann, D. Understanding TiO_2 Photocatalysis: Mechanisms and Materials. *Chem. Rev.* **2014**, *114*, 9919–9986. [CrossRef] [PubMed]

57. Wang, R.; Hashimoto, K.; Fujishima, K.; Chikuni, M.; Kojima, E.; Kitamura, A.; Shimohigoshi, M.; Watanabe, T. Light-induced amphiphilic surfaces. *Nature* **1997**, *388*, 431–432. [CrossRef]
58. Sakai, N.; Fujishima, A.; Watanabe, T.; Hashimoto, K. Enhancement of Photoinduced Hydrophilic Conversion Rate of TiO_2 Film Electrode Surface of Anodic Polarization. *J. Phys. Chem. B* **2001**, *105*, 3023–3026. [CrossRef]
59. Miyauchi, M.; Nakajima, A.; Watanabe, T.; Hashimoto, K. Photocatalysis and Photoinduced Hydrophilicity of Various Metal Oxide Films. *Chem. Mater.* **2002**, *14*, 2812–2816. [CrossRef]
60. Rtimi, S.; Pulgarin, C.; Sanjines, R.; Kiwi, J. Innovative semi-transparent nanocomposite films presenting photo-switchable behavior and leading to a reduction of the risk of infection under sunlight. *RSC Adv.* **2013**, *3*, 16345–16349. [CrossRef]
61. Rtimi, S.; Sanjines, R.; Pulgarin, C.; Kulik, A.; Kiwi, J. Innovative transparent non-scattering TiO_2 bactericide films inducing increased *E. coli* cell fluidity. *Surf. Coat. Technol.* **2014**, *254*, 333–343. [CrossRef]
62. Pulgarin, C.; Kiwi, J.; Nadtochenko, V. Mechanism of the photocatalytic destruction of bacteria by TiO_2 films leading to cell-wall damages and bacterial lysis. *Appl. Catal. B* **2012**, *128*, 179–183. [CrossRef]
63. Jayachandran, Y.; Narayandass, S. The effect of thickness of Ti-nitride coatings on bacterial adhesion. *Trends Biomater. Artif. Organs* **2010**, *24*, 90–93.
64. Rio, L.; Kusiak, E.; Kiwi, J.; Pulgarin, C.; Trampuz, C.; Bizzini, A. Comparative methods to evaluate the bactericidal activity of copper-sputtered surfaces against methicillin-resistant *Staphylococcus aureus*. *Appl. Environ. Microbiol.* **2012**, *78*, 8176–8182. [CrossRef] [PubMed]
65. Poole, R.; Kumar, I.; SalmonI, I.; Chance, B. The 650 and chromophore in *Escherichia coli* is oxy oxygenated compound, not the oxidized form of cytochrome oxidase: An hypothesis. *J. Gen. Microbiol.* **1983**, *129*, 1335–1344. [CrossRef] [PubMed]
66. Van Loosdrecht, L.; Lyklema, M.; Norde, W.; Schraa, G.; Zender, A. The role of bacterial cell-wall hydrophobicity in adhesion. *Appl. Environ. Microbiol.* **1987**, *53*, 1893–1990. [PubMed]
67. Xu, L.; Wellia, D.; Amal, R.; Liao, W.; Loo, J.; Tan, T. Fabrication of Highly Ordered TiO_2 Nanorod/Nanotube Adjacent Array for Photo-electrochemical Applications. *Langmuir* **2010**, *2*, 1122–1128.
68. Hogt, A.; Dankert, J.; Feijen, J. Adhesion of *Staphyloccocus epidermis* and *Staphyloccocus Saprophyticus* to a hydrophobic biomaterial. *J. Gen. Microbiol.* **1985**, *131*, 2485–2491. [PubMed]
69. Fletcher, R.; Loeb, M. Influence of the substratum characteristics on the attachment of a marine pseudomonas to solid surfaces. *Appl. Environ. Microbiol.* **1979**, *37*, 67–72. [PubMed]
70. Loveland, P.; Ryan, J.; Amy, G.; Harvey, R. The reversibility of virus attachment to mineral surfaces. *Colloid Surf. A Physicochem. Eng. Aspects* **1996**, *107*, 205–221. [CrossRef]
71. Zhukova, L.; Kiwi, J.; Nikandrov, V. Effect of the nanoparticles on *Escherichia coli* cell division capacity at pH 4–4.5 in the absence of UV-irradiation. *J. Colloids Surf. Bio-Interfaces* **2012**, *97*, 240–247. [CrossRef] [PubMed]
72. Nesic, J.; Rtimi, R.; Hebert, C.; Pulgarin, C.; Roglic, G.; Kiwi, J. New evidence for TiO_2 uniform surfaces leading to complete bacterial reduction in the dark: Critical issues. *Colloids Surf. B Biointerfaces* **2014**, *123*, 593–599. [CrossRef] [PubMed]
73. Kaegi, R.; Ulrich, B.; Sinnet, R.; Vonbank, R.; Wichser, A.; Zuleeg, S.; Simler, S.; Brunner, H.; Vonmont, H.; Burkhart, M.; et al. Synthetic TiO_2 nanoparticle emission from exterior facades into the aquatic environment. *Environ. Pollut.* **2008**, *156*, 233–239. [CrossRef] [PubMed]
74. Gottschalk, F.; Sonderer, T.; Scholz, W.; Nowack, B. Modeled Environmental Concentrations of Engineered Nanomaterials (ENM) for different regions and at different resolutions. *Environ. Sci. Technol.* **2009**, *43*, 9216–9222. [CrossRef] [PubMed]
75. Tong, T.; Shereef, A.; Wu, J.; Binh, C.; Kelly, J.; Gaillard, J.; Gray, K. Effects of the material morphology on the phototoxicity of nano-TiO_2 to bacteria. *Environ. Sci. Technol.* **2013**, *49*, 8113–8123. [CrossRef] [PubMed]
76. Lewinski, N.; Colvin, V.; Drezek, R. Cytotoxicity of Nanoparticles. *Small* **2008**, *4*, 26–49. [CrossRef] [PubMed]
77. Rincon, A.G.; Pulgarin, C. Photocatlytical inactivation of *E. coli*: Effect of the continuous-intermittent light intensity and of suspended fixed TiO_2 concentration. *Appl. Catal. B* **2003**, *44*, 263–284. [CrossRef]
78. Rincon, A.G.; Pulgarin, C. Bactericidal action of illuminated TiO_2 on pure *Escherichia coli* and natural bacterial consortia: Post-irradiation events in the dark and assessment of the effective disinfection time. *Appl. Catal. B* **2004**, *112*, 99–112. [CrossRef]
79. Miyauchi, M.; Irie, H.; Liu, M.; Qiu, X.; Yu, H.; Sunada, K.; Hashimoto, K. Visible-Light-Sensitive Photocatalysis: Nanocluster-Grafted Titanium Dioxide for Indoor Environmental remediation. *J. Phys. Chem. Lett.* **2016**, *7*, 75–84. [CrossRef] [PubMed]

80. Yoriya, S.; Chumphu, A.; Pookmanee, P.; Laithong, W.; Thepa, S.; Songprakorp, R. Multi-layered TiO_2 films towards enhancement of *Escherichia coli* inactivation. *Materials* **2016**, *9*, 808. [CrossRef]
81. Rtimi, S.; Pulgarin, C.; Sanjines, R.; Kiwi, J. Kinetics and mechanism for transparent polyethylene-TiO_2 films mediated self-cleaning leading to MB dye discoloration under sunlight irradiation. *App. Cat. B Environ.* **2015**, *162*, 236–244. [CrossRef]
82. Dunlop, P.S.M.; McMurray, T.A.; Hamilton, J.W.; Byrne, J.A. Inactivation of clinically relevant pathogens by photocatalytic coatings. *Photochem. Photobiol. A* **2010**, *196*, 113–119. [CrossRef]
83. McCullagh, C.; Robertson, C.; Bahnemann, D.; Robertson, K. The application of TiO_2 photocatalysisfor disinfection of water contaminated with pathogenic micro-orgnisms: A review. *Res. Chem. Intermed.* **2007**, *33*, 359–375. [CrossRef]
84. Amenazaga-Madrid, P.; Silveyra-Morales, R.; Cordoba-Fierro, L.; Orianda-Borunda, E.; Soli, J. TEM evidence of ultrastructural alteration on *Pseudomonas aeruginosa* by photocatlytic TiO_2 thin films. *J. Photochem. Photobiol. B* **2003**, *70*, 45–50. [CrossRef]
85. Mendez-Hermida, F.; Ares-Mazas, E.; McGuigan, G.; Boyle, M.; Sichel, C.; Fernandez-Ibanez, P. Disinfection of drinking water contaminated with *Crystosporidium parvum* oocysts under natural sunlight and using the photocatlyst TiO_2. *J. Photochem. Photobiol. B* **2007**, *66*, 105–111. [CrossRef] [PubMed]
86. Watts, J.; Kong, S.; Orr, P.; Miller, C.; Henry, E. Photocatalytic inactivation of coliform bacteria and viruses in secondary waste water effluents. *Water Res.* **1995**, *29*, 95–100. [CrossRef]
87. Lincous, A.; Carter, J.; Locuson, B.; Oulette, J.; Slattery, K.; Smith, A. Photocatalytic inhibition of algae growth using TiO_2, WO_3 and cocatalysts modifications. *Environ. Sci. Technol.* **2000**, *34*, 4752–4758. [CrossRef]
88. Sichel, C.; de Cara, M.; Tello, J.; Blanco, J.; Fernandez-Ibanez, P. Solar photocatalytic disinfection of agricultural pathogenic fungi: Fusarium species. *Appl. Catal. B* **2007**, *74*, 152–160. [CrossRef]
89. Kuhn, P.; Chaberny, F.; Massholder, K.; Stickler, M.; Benz, W.; Sonntag Gerdinger, L. Disinfection of surfaces by photocatalytic oxidation with titanium oxide und UV-light. *Chemosphere* **2003**, *53*, 51–57. [CrossRef]
90. Zhang, L.; Dillert, R.; Bahnemann, D.; Vormoor, M. Photo-induced hydrophilicity and self-cleaning: Models and reality. *Energy Environ. Sci.* **2012**, *5*, 7491–7507. [CrossRef]
91. Nakano, T.; Baba, S. Gas pressure effects on thickness uniformity and circumvented deposition during sputter deposition. *Vacuum* **2006**, *80*, 647–840. [CrossRef]
92. Dunill, C.W.; Aiken, Z.A.; Pratten, M.; Wilson, M.; Parkin, P.I. Sulfur- and Nitrogen-Doped Titania Biomaterials via APCVD. *Chem. Vap. Depos.* **2010**, *16*, 50–54. [CrossRef]
93. Evans, P.; Sheel, D. Photoactive and Antibacterial Thin Films on Stainless Steel. *Surf. Coat. Technol.* **2007**, *201*, 9319–9324. [CrossRef]
94. Foster, H.A.; Sheel, D.W.; Shel, P.; Evans, P.; Varghese, S.; Rutschke, N.; Yates, M.H. Antimicrobial activity of titania/silver and titania/copper films prepared by CVD. *J. Photochem. Photobiol. A* **2010**, *216*, 283–289. [CrossRef]
95. Caputo, G.; Nobile, C.; Buonsanti, R.; Lipp, T.; Manna, L.; Cingolani, R.; Cozzoli, P.; Atanssiou, A. Determination of surface properties of various substrates using TiO_2 nano-rod coatings with tunable characteristics. *J. Mater. Sci.* **2008**, *43*, 3474–3480. [CrossRef]
96. Irie, H.; Washizuka, S.; Hashimoto, K. Hydrophilicity on carbon-doped TiO_2 thin films under visible light. *Thin Solid Films* **2006**, *510*, 21–25. [CrossRef]
97. Scanlon, D.; Dunnill, W.D.; Buckeridge, J.; Shevlin, S.; Logsdail, S.; Scott, S.; Woodley, M.; Richard, C.; Catlow, A.; Powell, M.; et al. Band alignment of rutile and anatase TiO_2. *Nat. Mater.* **2013**, *12*, 798–801. [CrossRef] [PubMed]
98. Carneiro, J.; Teixeira, V.; Portinha, A.; Magalhães, A.; Newton, R.; Coutinho, P. Iron-doped photocatalytic TiO_2 sputtered coatings on plastics for self-cleaning applications. *Mater. Sci. Eng. B* **2007**, *138*, 144–150. [CrossRef]
99. Miron, C.; Roca, A.; Cozorici, P.; Sirghi, L. Photo-induced bactericidal activity activity of TiO_2 tin films obtained by radiofrequency magnetron sputtering deposition. *J. Optoelectr. Adv. Mater.* **2004**, *7*, 915–919.
100. Plowman, R.; Graves, R.; Griffin, N.; Taylor, L. The rate of added cost of hospital acquired infections. *J. Hosp. Infect.* **2001**, *47*, 198–204. [CrossRef] [PubMed]
101. Rossnagel, S.; Hopwood, J. Magnetron sputter deposition with high levels of metal ionization. *Appl. Phys. Lett.* **1993**, *63*, 3285–3287. [CrossRef]

102. Kelly, P.J.; Arnell, D.R. Magnetron sputtering: A review of recent developments and applications. *Vacuum* **2000**, *56*, 159–172. [CrossRef]
103. Sarakinos, K.; Alami, J.; Konstantinidis, S. High power pulsed magnetron sputtering: A review on scientific and engineering state of the art. *Surf. Coat. Technol.* **2010**, *204*, 1661–1684. [CrossRef]
104. Kousznetsov, V.; Macak, K.; Schneider, J.; Helmersson, U.; Petrov, I. A novel pulsed magnetron sputter technique utilizing very high target power densities. *Surf. Coat. Technol.* **1999**, *122*, 290–293. [CrossRef]
105. Castro, C.; Pulgarin, C.; Osorio, P.; Giraldo, S.; Kiwi, J. Structure-reactivity relations of the Cu-cotton sputtered layers during *E. coli* inactivation in the dark and under light. *J. Photochem. Photobiol. A* **2010**, *216*, 295–302. [CrossRef]
106. Osorio, P.; Sanjines Ruales, C.; Castro, C.; Pulgarin, C.; Rengifo, J.-A.; Lavanchy, J.-A.; Kiwi, J. Antimicrobial Cu-functionalized surfaces prepared by bipolar asymmetric DC-pulsed magnetron sputtering (PMS). *J. Photochem. Photobiol. A* **2011**, *220*, 70–76. [CrossRef]
107. Rtimi, S.; Baghriche, O.; Pulgarin, C.; Lavanchy, J.-C.; Kiwi, J. Growth of TiO_2/Cu films by HIPIMS for accelerated bacterial loss of viability. *Surf. Coat. Technol.* **2013**, *232*, 804–813. [CrossRef]
108. Li, C.; Tian, X.; Gong, C.; Xu, J. The improvement of high power impulse magnetron sputtering performance by an external unbalanced magnetic field. *Vacuum* **2016**, *133*, 98–104. [CrossRef]
109. Nikaido, H.J. Prevention of Drug Access to Bacterial Targets. Permeability Barriers and Active Flux. *Biol. Chem.* **1994**, *269*, 3905–3909.
110. Borkow, G.; Gabbay, J. Putting copper into action: Copper impregnated products with potential biocidal activities. *J. FASEB* **2008**, *18*, 1728–1730. [CrossRef] [PubMed]
111. Borkow, G.; Gabbay, J. Biocidal Textiles can help fight nosocomial infections. *Med. Hypothesis* **2008**, *70*, 990–994. [CrossRef] [PubMed]
112. Borkow, G.; Gabbay, J.; Dardik, R.; Eidelman, A.; Lavie, Y.; Grinfeld, Y.; Ikher, S.; Huszar, M.; Zatcoff, R.; Marikovsky, M. Molecular Mechanisms of enhanced wound healing by copper oxide-impregated dressing. *Wound Rep. Reg.* **2010**, *18*, 266–275. [CrossRef] [PubMed]
113. Borkow, G.; Gabbay, J. Copper an Ancient Remedy Returning to Fight Microbial, Fungal and Viral Infections. *Curr. Chem. Biol.* **2009**, *3*, 272–278. [CrossRef]
114. Applerot, G.; Abu-Mukh, R.; Irzh, R.; Charmet, J.; Keppner, J.; Laux, L.; Guilbert, G.; Gedanken, A. Decorative parylene coated glass with ZnO nano-particles for antibacterial applications. *ACS Appl. Mater. Interfaces* **2010**, *2*, 1052–1059. [CrossRef] [PubMed]
115. Perelshtein, I.; Applerot, N.; Perkas, N.; Wehrshuetz-Sigl, E.; Hasman, E.G.; Guebitz, G.; Gedanken, A. CuO-cotton nanocomposite: Formation, Morphology and bacterial activity. *Surf. Coat. Technol.* **2009**, *204*, 54–57. [CrossRef]
116. Torres, A.; Ruales, C.; Pulgarin, C.; Aimable, A.; Bowen, P.; Kiwi, J. Enhanced Inactivation of *E. coli* by RF-plasma Pre-treated Cotton/CuO (65 m^2/g) under Visible Light. *Appl. Mater. Interfaces* **2010**, *1*, 2547–2552. [CrossRef] [PubMed]
117. Kusiak-Nejman, E.; Morawski, A.; Ehiasarian, A.; Baghriche, O.; Pulgarin, C.; Mielczarski, E.; Mielczarski, J.; Kulik, A.; Kiwi, J. *E. coli* Inactivation by High Power Impulse Magnetron Sputtered (HIPIMS) Cu-Surfaces. *J. Phys. Chem. C* **2011**, *115*, 21113–21119. [CrossRef]
118. Haenle, M.; Fritsche, M.; Zietz, C.; Bader, M.; Heidenau, F. An extended spectrum bactericidal titanium dioxide (TiO_2) coating for metallic implants: In vitro effectiveness against MRSA and mechanical properties. *J. Mater. Sci. Mater. Med.* **2011**, *22*, 381–387. [CrossRef] [PubMed]
119. Rtimi, S.; Pulgarin, C.; Bensimon, M.; Kiwi, J. New Evidence for Cu-decorated binary-oxides mediating the bacterial inactivation/mineralization in aerobic media. *Colloids Surf. B Biointerfaces* **2016**, *144*, 222–228. [CrossRef] [PubMed]
120. Mathews, I. *Epitaxial Growth, Part B*; IBM Academic Press: New York, NY, USA, 1975; pp. 382–436.
121. Ehasarian, P.A. High-power impulse magnetron sputtering and its applications. *Pure Appl. Chem.* **2010**, *82*, 1247–1258. [CrossRef]
122. Rtimi, S.; Pulgarin, C.; Baghriche, O.; Kiwi, J. Accelerated inactivation obtained by HIPIMS sputtering on low cost surfaces with concomitant reduction in the metal-semiconductor content. *RSC Adv.* **2013**, *3*, 13127–13130. [CrossRef]
123. Mishra, A.; Kelly, J.-P.; Bradley, W.-J. The 2D-plasma potential distribution in a HIPIMS discharge. *J. Appl. Phys D Appl. Phys.* **2011**, *44*, 425201. [CrossRef]

124. Von Keudell, A.; Hecimovic, A.; Maszl, C. Control of High Power Pulsed Magnetron Discharge by Monitoring the Current Voltage Characteristics. *Contrib. Plasma Phys.* **2016**, *56*, 918–926. [CrossRef]
125. Petrov, I.; Myers, J.E.; Green, J.R.; Abelson, J. Mass and energy resolved detection of ions and neutral sputtered species incident at the substrate during reactive magnetron sputtering of Ti in mixed Ar+N_2 mixture. *J. Vac. Sci. Technol. A* **1994**, *12*, 2846–2851. [CrossRef]
126. Kousznetsov, V.; Mazak, K.; Schneider, J.; Helmersson, U.; Petrov, I. Ionized sputter-deposition using an extremely high plasma density pulsed magnetron discharge. *Surf. Coat. Technol.* **1999**, *12*, 20–295.
127. Song, Y.; Kwon, Y.; Choi, G.; Lee, W. Photocatalyric activity of Cu/TiO_2 with oxidation state of surface loaded copper. *Bull. Korean Chem. Soc.* **1999**, *20*, 957–960.
128. Yu, J.; Ran, J. Facile preparation and enhanced photocatlytic activity H_2-production activity of $Cu(OH)_2$ cluster modified TiO_2. *Energy Environ. Sci.* **2011**, *4*, 1364–1371. [CrossRef]
129. Lopez-Ayala, S.; Rincon, E.M. Catalytic and photocatalytic performance of mesoporous Cu_xO-TiO_2. *J. Photochem. Photobiol. A* **2011**, *222*, 249–257. [CrossRef]
130. Rodriguez-Torres, C.; Golmar, F.; Cabrera, A.; Errico, L.; Mudara-Navarro, M.A.; Renteria, M.; Sanchez, F.; Duhalde, S. Magnetic and structural study of Cu-doped TiO_2 thin films. *Appl. Surf. Sci.* **2007**, *254*, 365–367. [CrossRef]
131. Audronis, M.; Hinder, S.; Mack, P.; Bellido-Gonzales, V.; Bussey, D.; Mathews, A.; Baker, M. A comparison of reactive plasma pretreatments on PET substrates by Cu and Ti pulsed-DC and HIPIMS discharges. *Thin Solid Films* **2011**, *520*, 1564–1570. [CrossRef]
132. Ballo, M.; Rtimi, S.; Mancini, S.; Kiwi, J. Bactericidal activity and mechanism of action of copper sputtered flexible surfaces against multidrug-resistant pathogens. *Appl. Microbiol. Cell Physiol.* **2016**, *100*, 5945–5953. [CrossRef] [PubMed]
133. Warnes, S.L.; Keevil, C.W. Mechanism of copper surface toxicity in vancomycin-resistant enterococci following wet or dry surface contact. *Appl. Environ. Microbiol.* **2011**, *77*, 6049–6059. [CrossRef] [PubMed]
134. Sands, K.; Vineyard, G.; Platt, R. Surgical site infections occurring after hospital discharge. *J. Infect. Dis.* **1996**, *173*, 963–970. [CrossRef] [PubMed]
135. Gharsa, H.; Dziri, R.; Klibi, N.; Chairat, S.; Lozano, C.; Torres, C.; Bellaaj, R.; Ben Slama, K. Environmental *Staphylococcus aureus* contamination in a Tunisian hospital. *J. Chemother.* **2016**, *28*, 506–509. [CrossRef] [PubMed]
136. Quaranta, D.; Krans, T.; Espirito Santo, C.; Elowsky, C.; Domaille, D.; Chang, C.; Grass, G. Mechanisms of contact-mediated killing of yeast cells on dry metallic copper surfaces. *Appl. Environ. Microbiol.* **2011**, *77*, 416–426. [CrossRef] [PubMed]
137. Espirito Santo, C.; Lam, E.; Elowsky, C.; Quaranta, D.; Domaille, D.; Chang, C.; Grass, G. Bacterial killing by dry metallic copper surfaces. *Appl. Environ. Microbiol.* **2011**, *77*, 794–802. [CrossRef] [PubMed]
138. Grass, G.; Rensing, C.; Solioz, M. Metallic copper as an antimicrobial surface. *Appl. Environ. Microbiol.* **2011**, *77*, 1541–1547. [CrossRef] [PubMed]
139. Casey, A.L.; Adams, D.; Karpanen, T.J.; Lambert, P.A.; Cookson, B.D.; Nightingale, P.; Miruszenko, L.; Shilla, R.; Christian, P.; Elliot, T.S. Role of copper in reducing hospital environment contamination. *J. Hosp. Infect.* **2010**, *74*, 72–77. [CrossRef] [PubMed]
140. Heidenau, F.; Mittelmeir, W.; Detsch, R.; Haenle, M.; Stenzel, F.; Ziegler, G. A novel antibacterial titania coating: Metal ion toxicity in vitro surface colonization. *J. Mater. Sci. Med.* **2005**, *16*, 883–888. [CrossRef] [PubMed]
141. Edgeworth, J. Intravascular catheter infections. *J. Hosp. Infect.* **2010**, *73*, 323–330. [CrossRef] [PubMed]
142. O'Grady, N.P.; Alexander, M.; Burns, L.A.; Dellinger, E.P.; Garland, J.; Heard, S.O.; Lipsett, P.A.; Masur, H.; Mermel, L.A.; Pearson, M.L.; et al. Guidelines for the prevention of intravascular catheter-related infections. *Clin. Infect. Dis.* **2011**, *52*, 162–193. [CrossRef] [PubMed]
143. Mermel, L.A. What is the predominant source of intravascular catheter infections? *Clin. Infect. Dis.* **2011**, *2*, 211–212. [CrossRef] [PubMed]
144. Tong, S.Y.; Davis, J.S.; Eichenberger, E.; Holland, T.L.; Fowler, V.G., Jr. Staphylococcus aureus infections: Epidemiology, pathophysiology, clinical manifestations and management. *Clin. Microbiol. Rev.* **2015**, *28*, 603–661. [CrossRef] [PubMed]
145. Ballo, M.; Rtimi, S.; Pulgarin, C.; Hopf, N.; Berthet, A.; Kiwi, J.; Moreillon, P.; Entenza, J.; Bizzini, A. In vitro and in vivo effectiveness of an innovative silver-copper nanoparticle coating of catheters to prevent methicillin-resistant *Staphylococcus aureus* infection. *Antimicrob. Agents Chemother.* **2016**, *60*, 5349–5356. [CrossRef] [PubMed]

146. Weaver, L.; Noyce, J.; Michels, H.; Keeevil, C. Potential action of Cu surfaces on meticillin-resistant *Staphylococcus aureus*. *Appl. Microbiol.* **2010**, *109*, 2200–2205. [CrossRef] [PubMed]
147. Zietz, C.; Fritsche, A.; Finke, B.; Stranak, V.; Haenle, M.; Hippler, R.; Mittelmeier, W.; Bader, R. Analysis of the release characteristics of Cu-treated antimicrobial implants surface using atomic absorption spectrometry. *Bioorg. Chem. Appl.* **2012**, *2012*, 850390. [CrossRef] [PubMed]
148. Gunawan, C.; Teoh, W.; Matrquis, C.; Amal, R. Cytotoxyc Origin of Copper (II)Oxide Nanoparticles: Comparative Studies with Micron-Sized Particles, Leachate and Medical Salts. *ACS Nano* **2011**, *5*, 7214–7225. [CrossRef] [PubMed]
149. Bondarenko, O.; Juganson, K.; Ivask, A.; Kasemets, K.; Mortimer, M.; Kahru, A. Toxycity of Ag, CuO, and ZnO nanoparticles to selected environmentally relevant test organisms and mammalian cells in vitro: A critical review. *Arch. Toxicol.* **2013**, *87*, 1181–1200. [CrossRef] [PubMed]
150. Nguyen, T.; Park, H.; Kim, J.; Kim, H.; Lee, H.; Yoon, J.; Lee, C. Microbial inactivation by Cupric Ion in Combination with H_2O_2: Role of Reactive Oxidants. *Environ. Sci. Technol.* **2013**, *47*, 13661–13667. [CrossRef] [PubMed]
151. Gao, G.; Pang, H.; Xu, S.; Lu, Q. Copper based nanostructures: Promising antibacterial agents and photocatalysis. *Chem. Commun.* **2009**, 3571–3573. [CrossRef] [PubMed]
152. Gedanken, A.; Perkas, N.; Perelshtein, I.; Applerot, G.; Lipovsky, A.; Nitzan, Y.; Lubart, R. Chapter 9. Innovative Inorganic Nanoparticles with Antimicrobial Properties Attached to Textiles by Sonochemistry. In *Cavitation: A Novel Energy-Efficient Technique for the Generation of Nanomaterials*; Manickam, S., Ashokkumar, M., Eds.; Pan Stanford Publishing: Singapore, 2014; pp. 263–300.
153. Sedighi, A.; Montazer, M.; Samadi, N. Synthesis of nano-Cu_2O on cotton: Morphological, physical, biological and optical sensing characteristics. *Carbohydr. Polym.* **2014**, *110*, 489–498. [CrossRef] [PubMed]
154. Linder, M.C. The relationship of copper to DNA damage and damage prevention in humans. *Mutant. Res.* **2012**, *733*, 83–91. [CrossRef]
155. Irie, H.; Kamiya, K.; Shibanuma, T.; Miura, S.; Tryck, D.; Yo koyama, T.; Hashimoto, K. Visible light sensitive Cu(II)-grafted TiO_2 photocatalysts: Activities and X-ray absorption fine structure analyses. *J. Phys. Chem. C* **2009**, *113*, 10671–10766. [CrossRef]
156. Irie, H.; Miura, S.; Kamiya, K.; Hashimoto, K. Efficient visible light-sensitive photocatalysts: Grafting Cu(II) onto TiO_2 and WO_3 photocatalysts. *Chem. Phys. Lett.* **2008**, *457*, 202–205. [CrossRef]
157. Ishiguro, H.; Yao, Y.; Nakano, R.; Hara, M.; Sunada, K.; Hashimoto, K.; Kajioka, J.; Fujishima, A.; Kubota, Y. Photocatalytic activity of Cu^{2+}/TiO_2-coated cordierite foam inactivates bacteriophages and *Legionella pneumophila*. *Appl Catal. B* **2013**, *129*, 56–61. [CrossRef]
158. Yates, M.H.; Brook, L.A.; Ditta, B.I.; Evans, P.; Foster, H.A.; Sheel, W.D.; Steele, A. Photo-induced self-cleaning and biocidal bahavior of titania and copper oxide multilayers. *J. Photochem. Photoboiol. A* **2008**, *197*, 197–205. [CrossRef]
159. Kelly, J.P.; Li, H.; Benson, S.P.; Whitehead, K.A.; Verran, J.; Arnell, D.R.; Iordanova, I. Comparison of the tribological and antimicrobial propertiesof CrN/Ag, ZrN/Ag, TiN/Ag and TiN/Cu nancomposite coatings. *Surf. Coat Technol.* **2010**, *205*, 1606–1610. [CrossRef]
160. Caballero, L.; Whitehead, A.K.; Allen, S.N.; Verran, J. Inactivation of *Esherichia coli* on immobilized TiO_2 using fluorescent light. *J. Photochem. Photobiol. A* **2009**, *202*, 92–98. [CrossRef]
161. Kelly, P.J.; Barker, M.P.; Ostovarpour, S.; Ratova, M.; West, T.G.; Iordanova, I.; Bradley, W.J. Deposition of photocatalytic titania coatings on polymer substrates by HIPIMS. *Vacuum* **2012**, *86*, 1880–1882. [CrossRef]
162. Leyland, N.; Podporska, A.; Caroll, J.; Browne, J.; Hinder, S.; Quilty, B.; Pillai, C.S. Highly efficient F, Cu-doped TiO_2 antibacterial visible light active photocatalytic coatings to combat hospital acquired infections. *Nat. Sci. Rep.* **2016**, *6*, 24770. [CrossRef] [PubMed]
163. Ryan, D.; Pillai, S.C.; Carrol, J. Dublin Institute of Technology. A Surface Coating. U.S. Patent 9,210,934, 15 December 2015.
164. Baghriche, O.; Rtimi, S.; Pulgarin, C.; Sanjines, R.; Kiwi, J. Innovative TiO_2/Cu nanosurfaces inactivating bacteria in the minute range under low intensity actinic light. *ACS Appl. Mater. Interfaces* **2012**, *4*, 5234–5240. [CrossRef] [PubMed]
165. Jeng, J.H. Swanson, Toxicity of metal oxide nanoparticles in mammalian cells. *J. Environ. Sci. Health Part A Toxic. Hazard. Subst. Environ. Eng.* **2006**, *4*, 2699–2711. [CrossRef] [PubMed]

166. Baghriche, O.; Rtimi, S.; Pulgarin, C.; Sanjines, R.; Kiwi, J. Effect of the spectral properties of TiO_2, Cu, TiO_2/Cu sputtered films on the bacterial inactivation under low intensity actinic light. *J. Photochem. Photobiol. A* **2013**, *251*, 50–56. [CrossRef]
167. Kiwi, J.; Morrison, C. Heterogeneous photocatalysis. Dynamics of charge transfer in lithium-doped anatase-based catalyst powders with enhanced water photocleavage under ultraviolet irradiation. *J. Phys. Chem.* **1984**, *88*, 6146–6152. [CrossRef]
168. De Romanha, D.L.; Olivares, M.; Uauy, R.; Araya, M. Risks and benefits of copper in light of new insights of copper homeostasis. *J. Trace Elements Med. Biol.* **2011**, *25*, 3–13. [CrossRef] [PubMed]
169. Rtimi, S.; Ballo, M.; Laub, D.; Pulgarin, C.; Entenza, J.; Bizzini, A.; Kiwi, J. Duality in the *Eschericia coli* and methicillin resistant *Staphylococcus aureus* reduction mechanism under actinic light on innovative co-sputtered surfaces. *Appl. Catal. A* **2015**, *498*, 185–191. [CrossRef]
170. Qiu, X.; Miyauchi, M.; Sunada, K.; Minoshima, M.; Liu, M.; Lu, Y.; Ding, M.; Shomodara, Y.; Hosogi, Y.; Kuroda, Y.; et al. Hybrid Cu_x/TiO_2 nanocomposites as Risk-Reduction Materials in Indoor Environments. *ACS Nano* **2012**, *6*, 1609–1618. [CrossRef] [PubMed]
171. Grey, B.; Steck, R. Concentrations of Copper Thought to be Toxic to *Esherichia coli* Can Induce the Viable but Nonculturable Condition. *Appl. Environ. Microbiol.* **2001**, *67*, 5325–5327. [CrossRef] [PubMed]
172. Rtimi, S.; Pulgarin, C.; Sanjines, R.; Nadtochenko, V.; Lavanchy, J.-C.; Kiwi, J. Preparation and Mechanism of Cu-decorated TiO_2-ZrO_2 Films Showing Accelerated Bacterial Inactivation. *ACS Appl. Mater. Interfaces* **2015**, *7*, 12832–12839. [CrossRef] [PubMed]
173. Rtimi, S.; Pulgarin, C.; Sanjines, R.; Kiwi, J. Accelerated self-cleaning by Cu-promoted binary-oxides under sunlight. *Appl. Catal. B* **2016**, *180*, 648–655. [CrossRef]
174. Neubert, S.; Mitoraj, D.; Shevlin, S.; Pulisova, P.; Heimann, M.; Du, Y.; Gregory, C.; Goh, K.; Pacia, M.; Kruczał, K.; et al. Highly efficient rutile TiO_2 photocatalyst with single Cu(II) and Fe(III) surface catalytic sites. *J. Mater. Chem. A* **2016**, *4*, 3127–3133. [CrossRef]
175. Karunakaran, C.; Abiramasundari, G.; Gomathisankar, P.; Manikanda, G.; Anandi, V. Cu-doped TiO_2 nanoparticles for photocaatlytic disinfection of bacteria under visible light. *J. Colloid Interfaces Sci.* **2010**, *352*, 68–74. [CrossRef] [PubMed]
176. Warnes, S.; Green, S.; Michels, H.; Keevil, C. Biocidal efficacy of copper alloys against pathogenic enterococci involves degradation of genomic and plasmid DNAs. *Appl. Environ. Microbiol.* **2010**, *76*, 5390–5401. [CrossRef] [PubMed]
177. Eshed, M.; Lellouche, J.; Matalon, S.; Gedanken, A.; Banin, M. Sonochemical coatings of ZnO and CuO nanoparticles inhibit streptococcus mutans biofilm formation on teeth model. *Langmuir* **2012**, *28*, 12288–12295. [CrossRef] [PubMed]
178. Chang, S.; Liu, W. The roles of the surface-doped metal-ions (V, Mn, Fe, Cu, Ce, and W) in the interfacial behavior of TiO_2 photocatalysts. *Appl. Catal. B* **2014**, *156–157*, 466–475. [CrossRef]
179. Lemire, A.; Harrison, J.; Turner, R. Antimicrobial activity of metals: Mechanism, molecular targets and applications. *Nat. Rev. Microbiol.* **2013**, *11*, 371–384. [CrossRef] [PubMed]
180. Pham, T.; Lee, B. Disinfection of Sthphylococcus aureus in indoor aerosols using Cu-TiO_2 deposited on glassfibers under visible light irradiation. *J. Photochem. Photobiol. A* **2015**, *307–308*, 16–22. [CrossRef]
181. Liu, L.; Giu, X.; Sun, C.; Li, H.; Deng, Y.; Gao, F.; Dong, L. In situ loading of ultrasmall Cu_2O particles on TiO_2 nanosheets to enhance the visible light photoactivity. *Nanoscale* **2012**, *4*, 6351–6359. [CrossRef] [PubMed]
182. Musil, J. Flexible hard nanocomposite coatings. *RSC Adv.* **2015**, *5*, 60482–60495. [CrossRef]
183. Musil, J.; Blazek, J.; Fajfrlik, K.; Cerstvy, R. Flexible antibacterial Al-Cu-N films. *Surf. Coat. Technol.* **2015**, *264*, 114–120. [CrossRef]
184. Musil, J.; Karel, M.; Fajfrlik, K.; Cerstvy, R.J. Flexible antibacterial Zr-Cu-N thin films resistant to cracking. *Vac. Sci. Technol. A* **2015**, *34*. [CrossRef]